nanomechanics and mesoscopic phonons

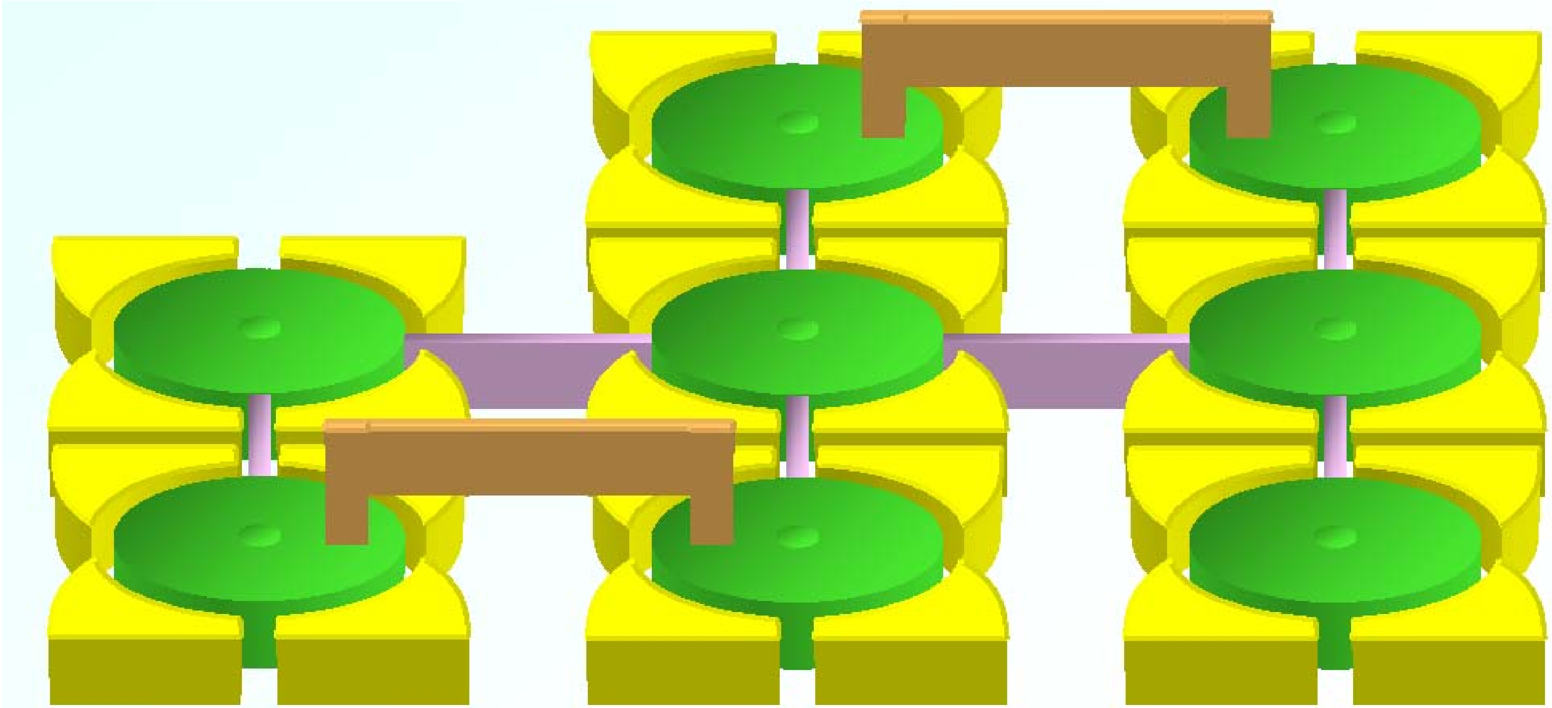

Integrated Mechanical Circuits

Courtesy CT-Cnyugen (Berkeley)

Why NEMS? Device applications

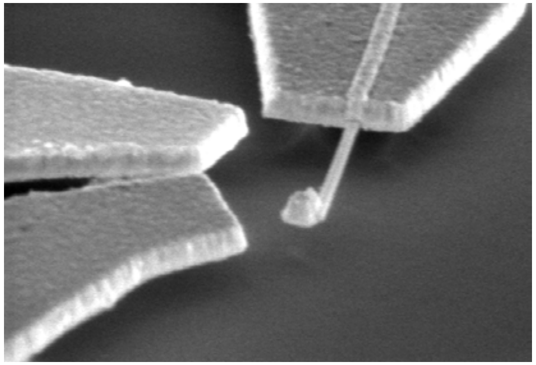

- Smaller, cheaper, faster, lower power consumption
- "Phones of the future": NEM-devices are in the right frequency range (1-5 GHz) to replace elements in cell phones
- Better frequency selectivity (higher Q)
- Bulk passive components replaced by smaller size MEMS/NEMS components
- New sensor applications

needed: high Q; high frequency

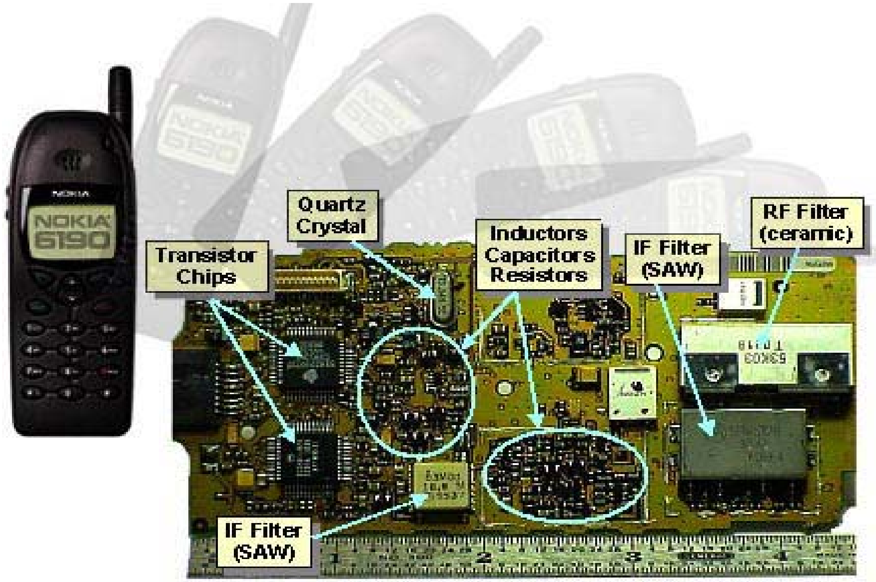

Nanotube RAM (including movie):
http://www.nantero.com/index.html

mass sensing on the level of single molecules

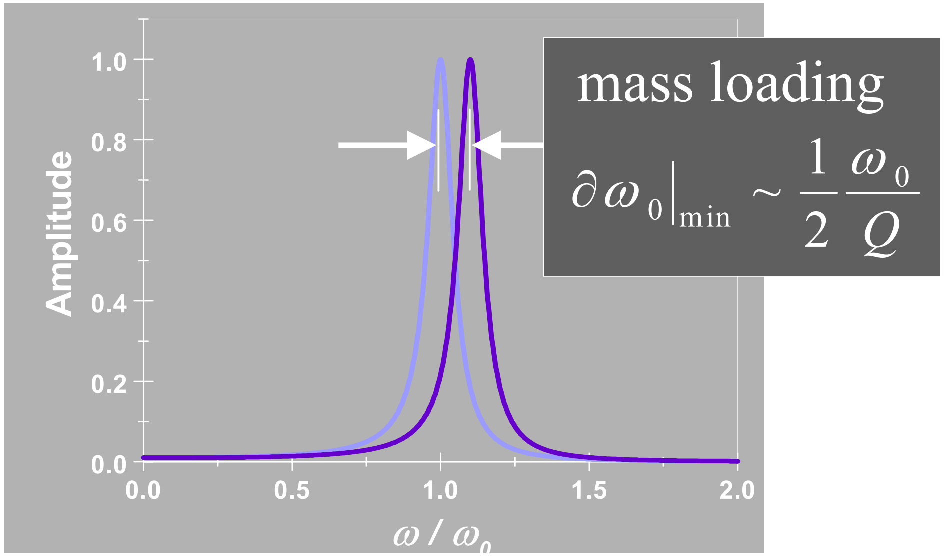

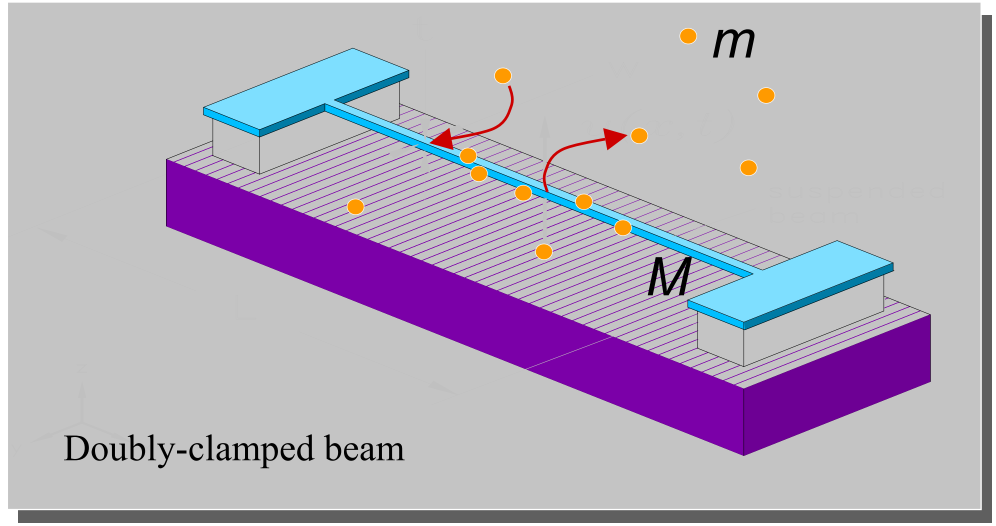

$$\partial M_{min} \approx m / Q$$

f_0	$L \times w \times t$ (μm)	M_{eff}	Q	∂m_{min} (d)
7.7 MHz	10 x 0.2 x 0.1	230 *fg*	10,000	1.4×10^8
"	"	"	100,000	1.4×10^7
380 MHz	1 x 0.05 x 0.05	3 *fg*	10,000	1.8×10^6
"	"	"	100,000	1.8×10^5
7.7 GHz	0.1 x 0.01 x 0.01	23 *ag*	10,000	1400
"	"	"	100,000	140

low *M* (high *f*); high *Q*

carbon-nanotube oscillators towards zeptogram detection

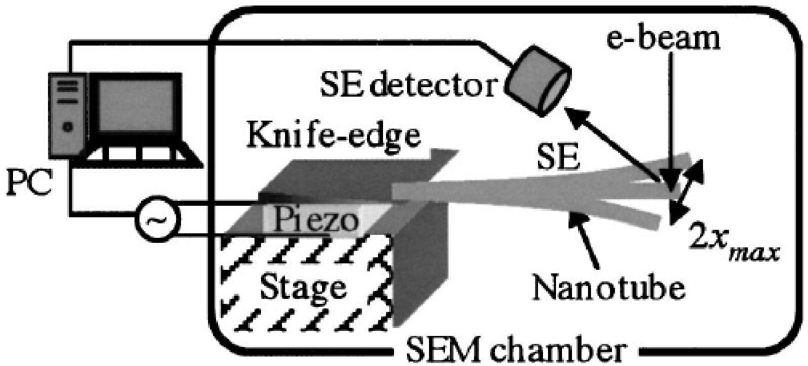

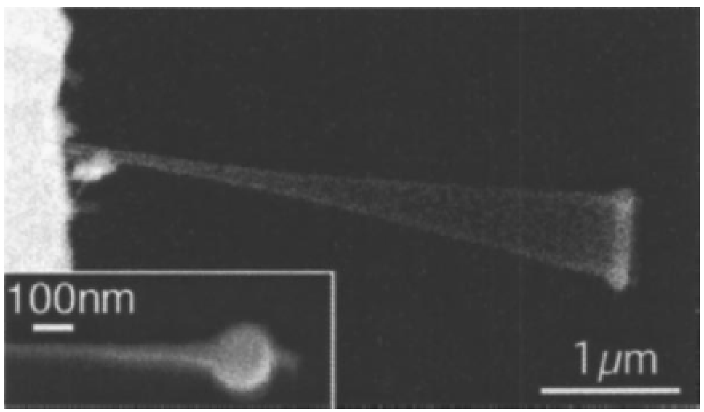

FIG. 2. SEM image of a carbon nanotube oscillator. The inset shows the deposit induced by an electron beam deposition process.

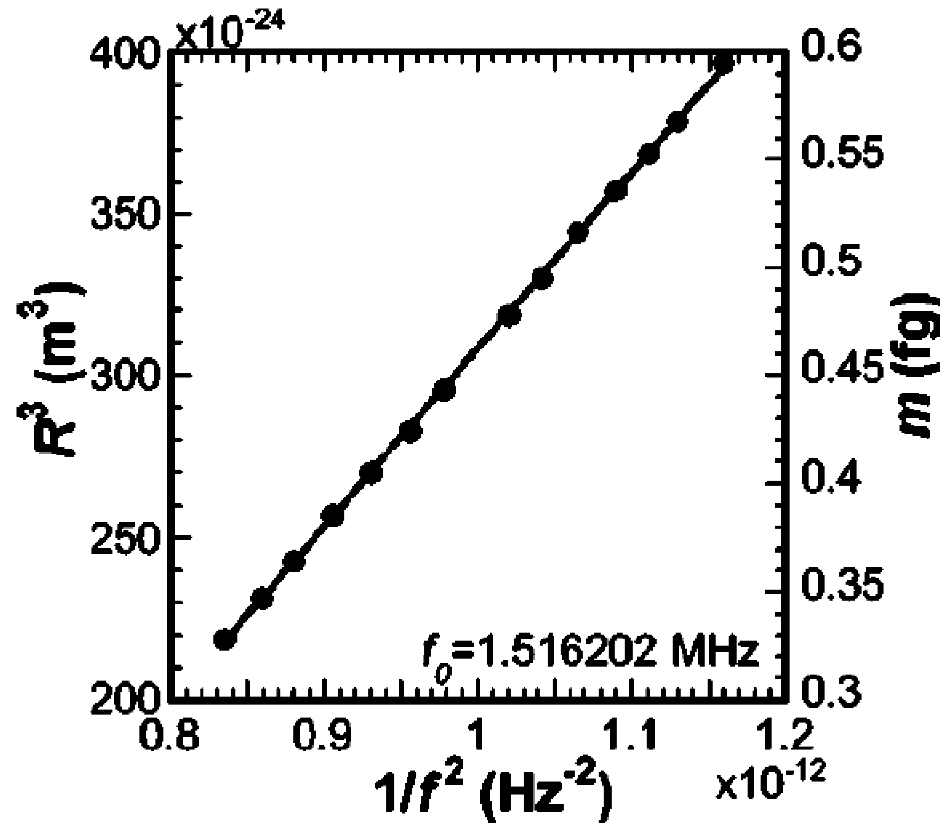

M. Nishio et al. APL 86 (2005) 133111

nanorelays: low-power mechanical switches

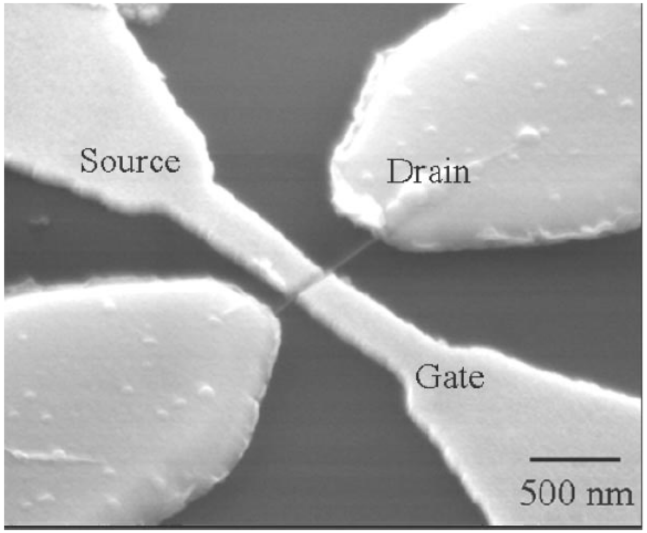

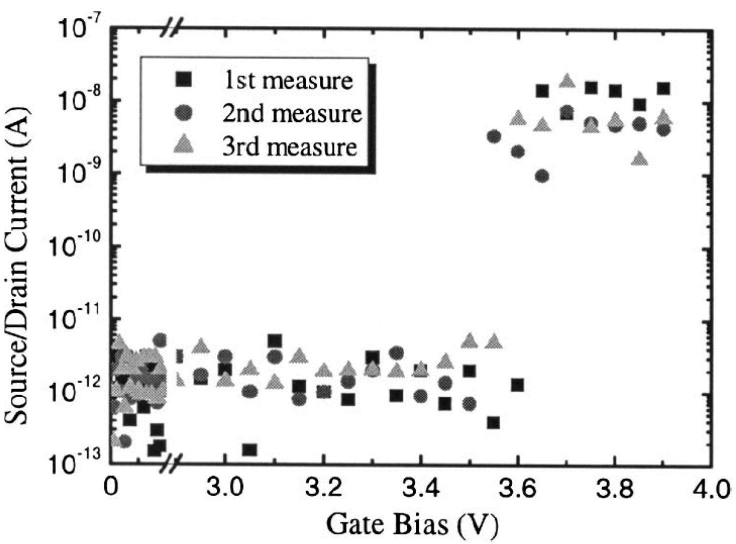

S.N. Cha et al. APL **86** (2005) 083105

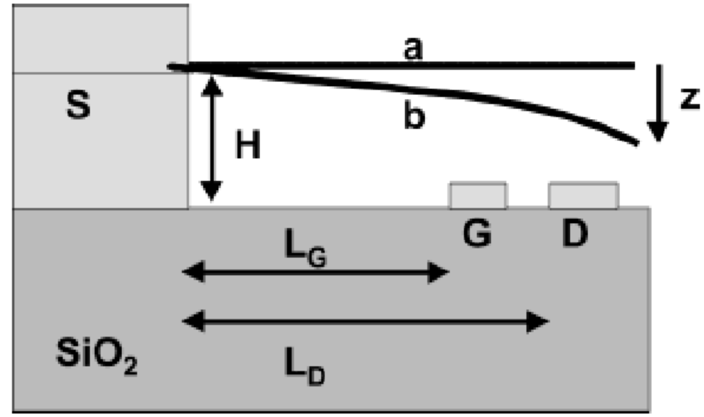

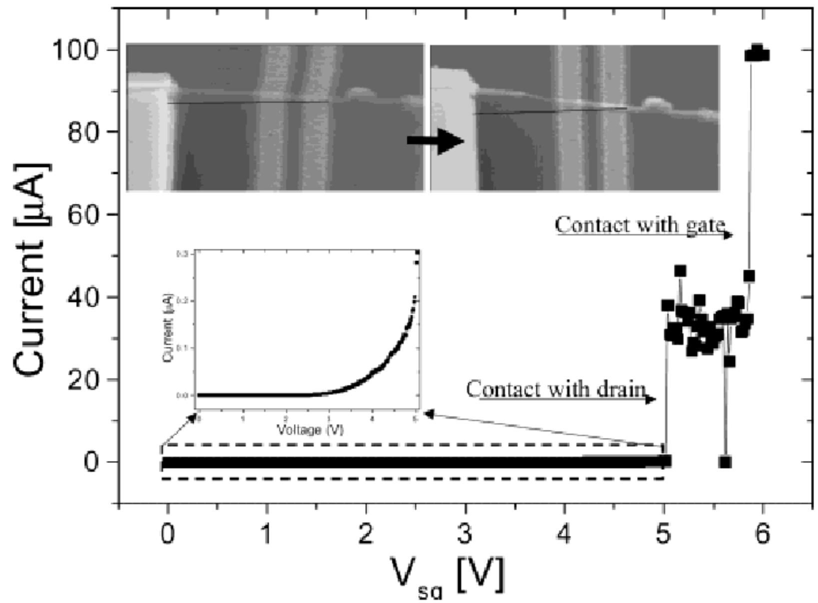

S.W. Lee et al. Nanoletters (2004)

nanotube-nanomechanics: rotator

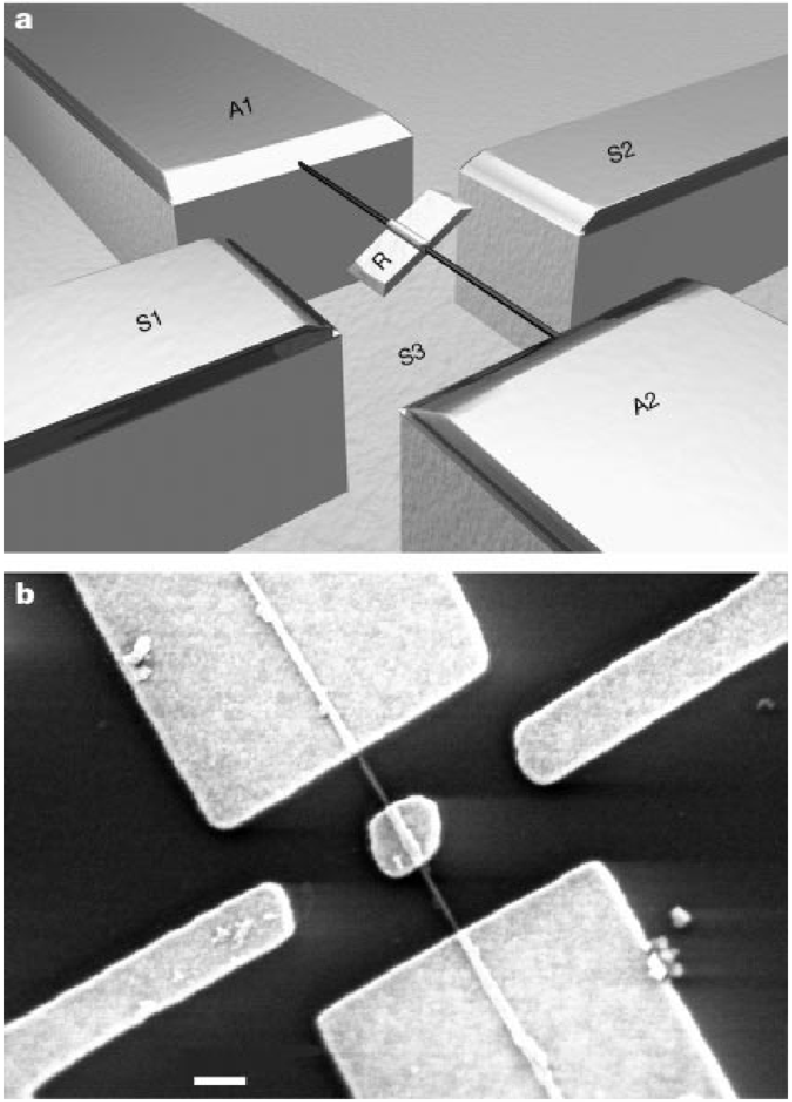

rotating mirror

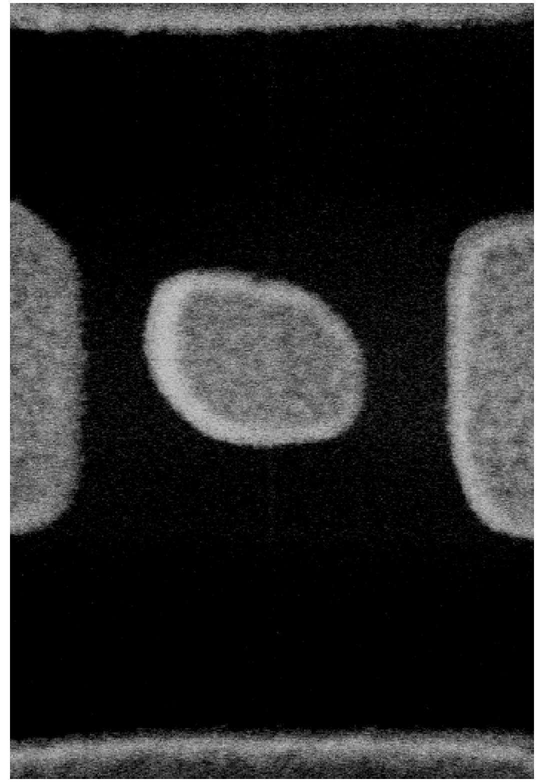

low-friction internal motion of the shells of a multi-wall nanotube makes motion possible

Fennimore et al, Nature ***286*** *(1999) 2148*

bio-nanomechanics II

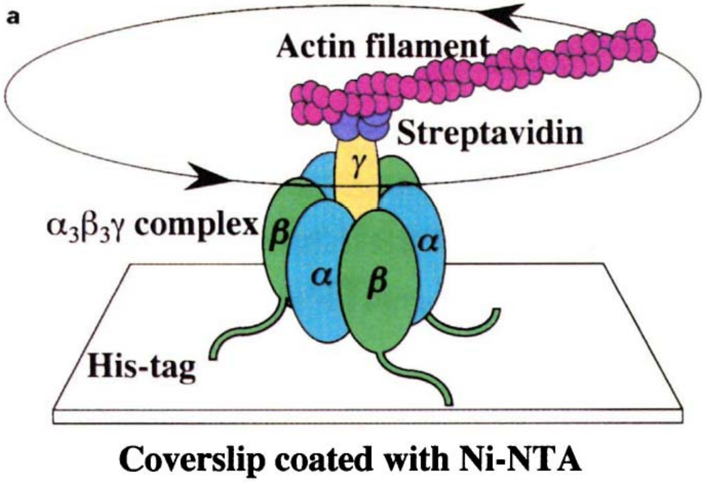

bio-motors: **ATP fuelled biomotor with a fluorescent filament of a few micron length attached (time between pictures 133 ms)**

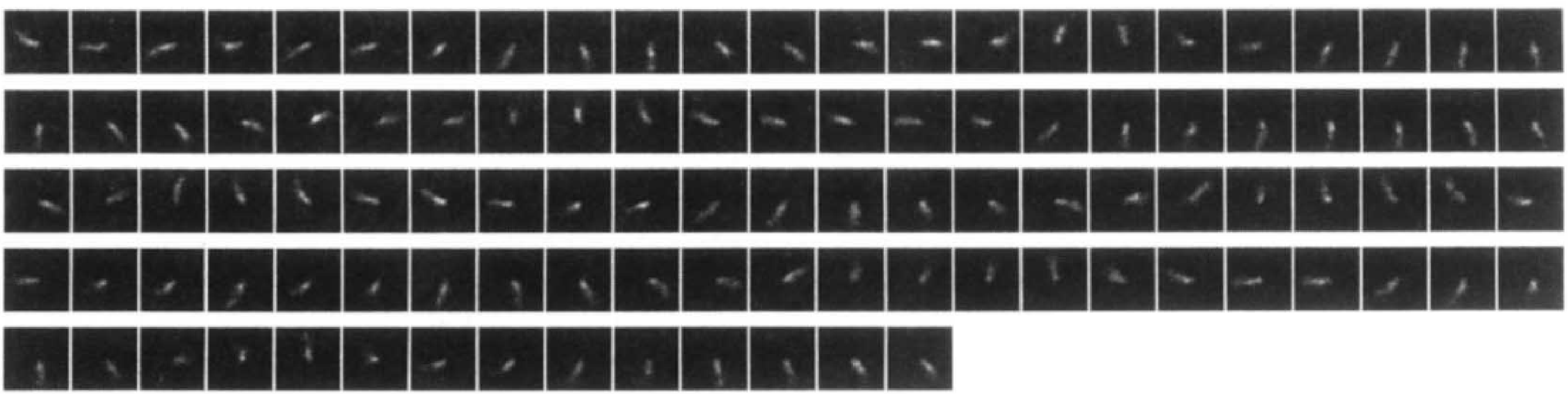

*H. Nori et al. Nature **386** (1997) 299*

nanomechanics of breaking an atomic gold wire

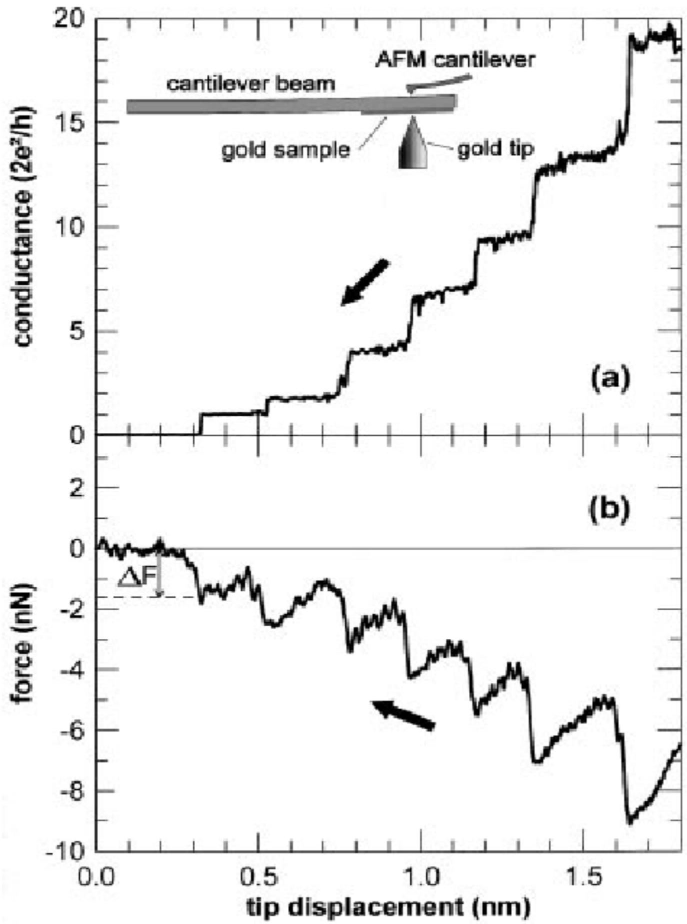

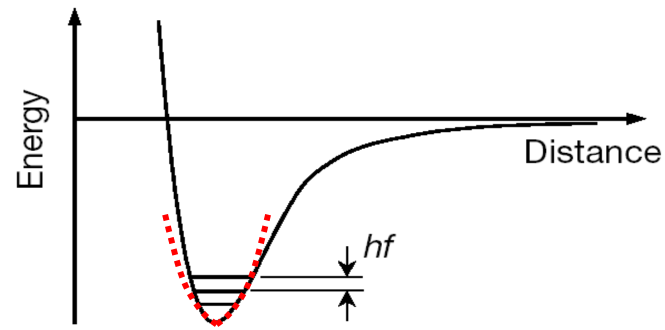

estimate force:

$$x_0 = 0.2\,\mathrm{nm}$$

$$E_b = 3\,\mathrm{eV}$$

$$k \approx \frac{\partial^2 V(x)}{\partial^2 x} \approx 10\,\mathrm{N/m}$$

$$F = \; k x_0 = 2\,\mathrm{nN}$$

G. Rubio et al., PRL 67 (1996) 2302

Measurement of the conductance of a hydrogen molecule

NATURE | VOL 419 | 31 OCTOBER 2002

R. H. M. Smit*, Y. Noat*†, C. Untiedt*, N. D. Lang‡, M. C. van Hemert§ & J. M. van Ruitenbeek*

* *Kamerlingh Onnes Laboratorium, Universiteit Leiden, PO Box 9504, 2300 RA Leiden, The Netherlands*
‡ *IBM Research Division, Thomas J. Watson Research Center, Yorktown Heights, New York 10598, USA*
§ *Leids Instituut voor Chemisch Onderzoek, Gorlaeus Laboratorium, Universiteit Leiden, PO Box 9502, 2300 RA Leiden, The Netherlands*

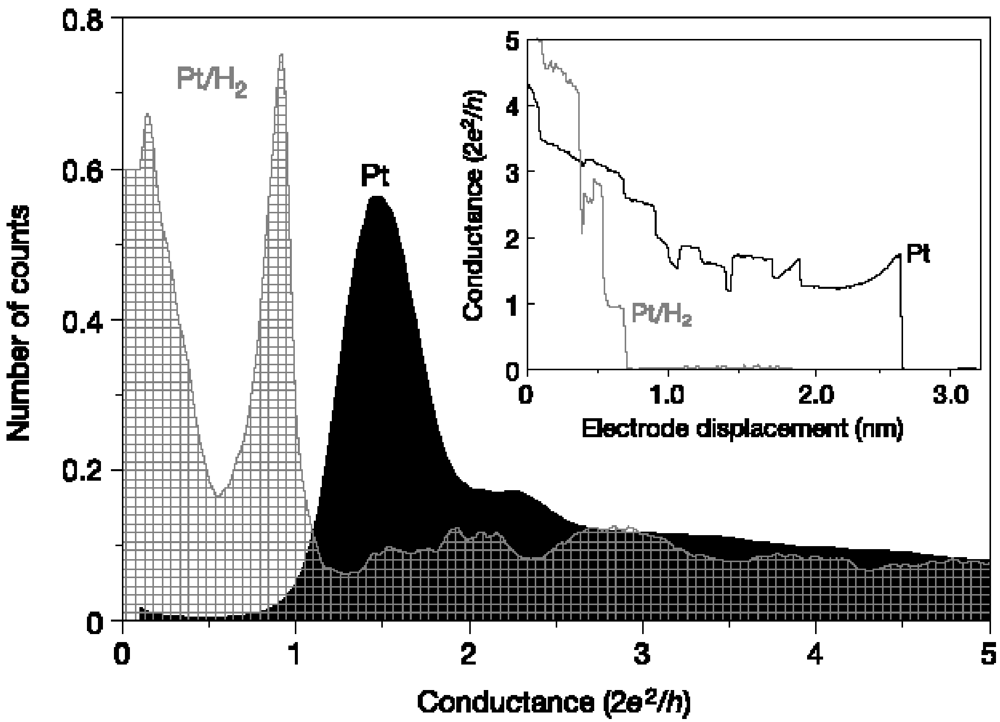

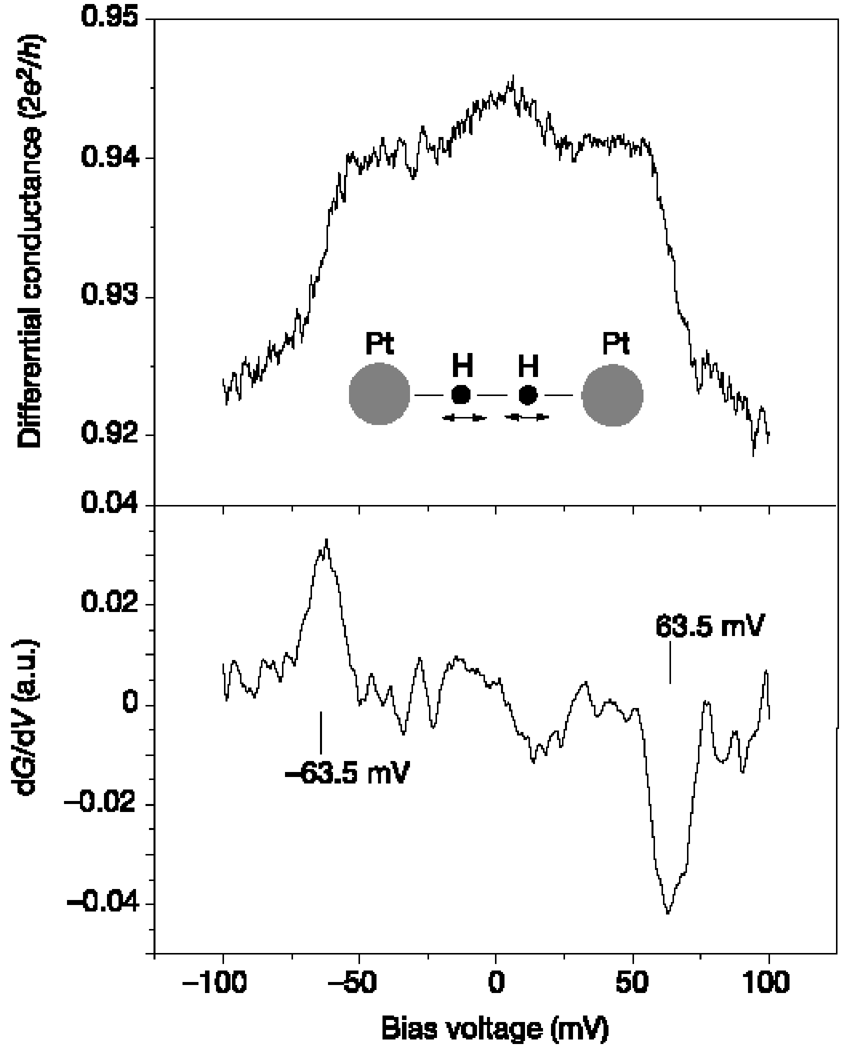

vibrational modes in Pt-H_2-Pt junctions

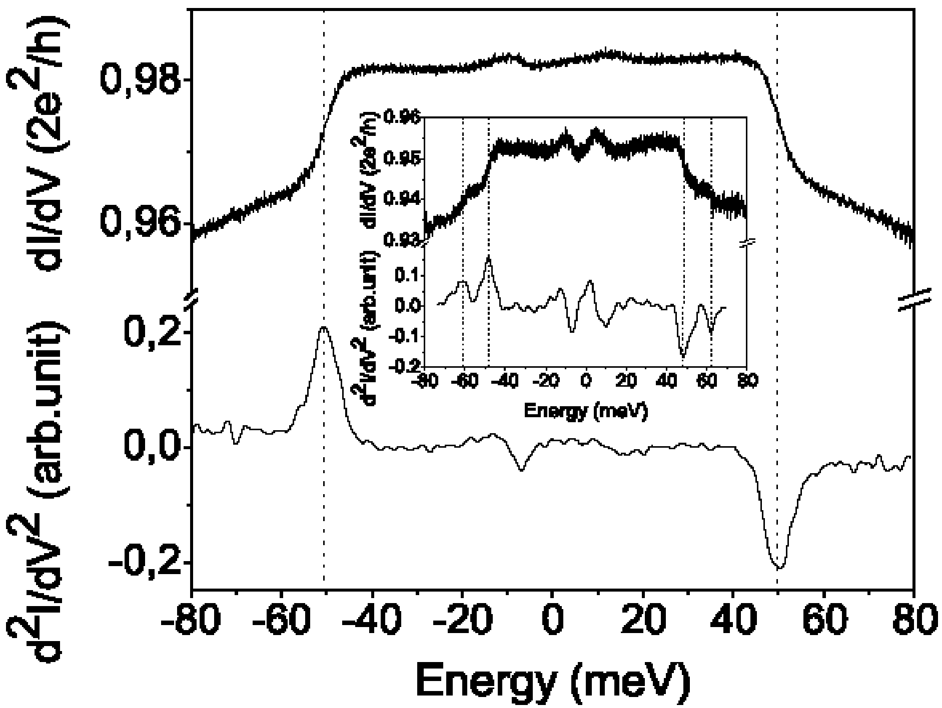

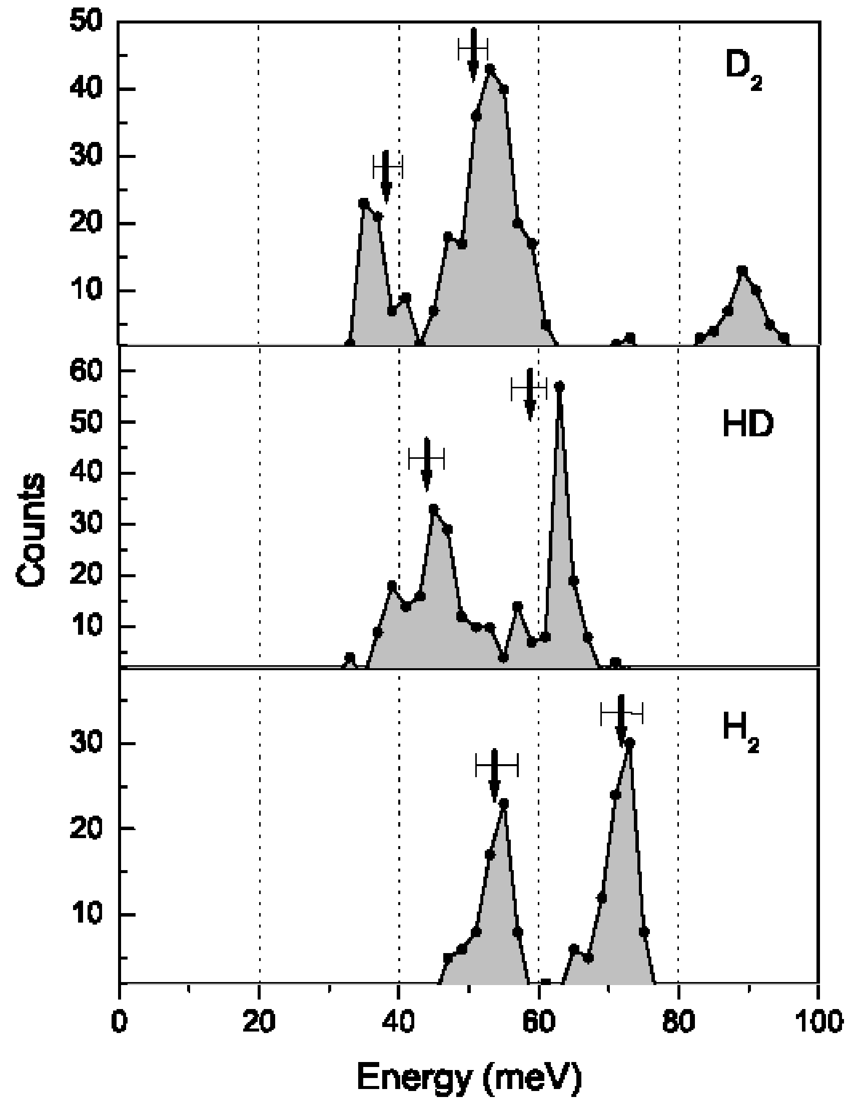

lithographic break junction
Inelastic tunneling spectroscopy (IETS)

Djukic et al. cond/mat 0409640

stretching the contact: longitudinal or transversal modes?

$$\omega = \sqrt{\frac{k}{m}}$$

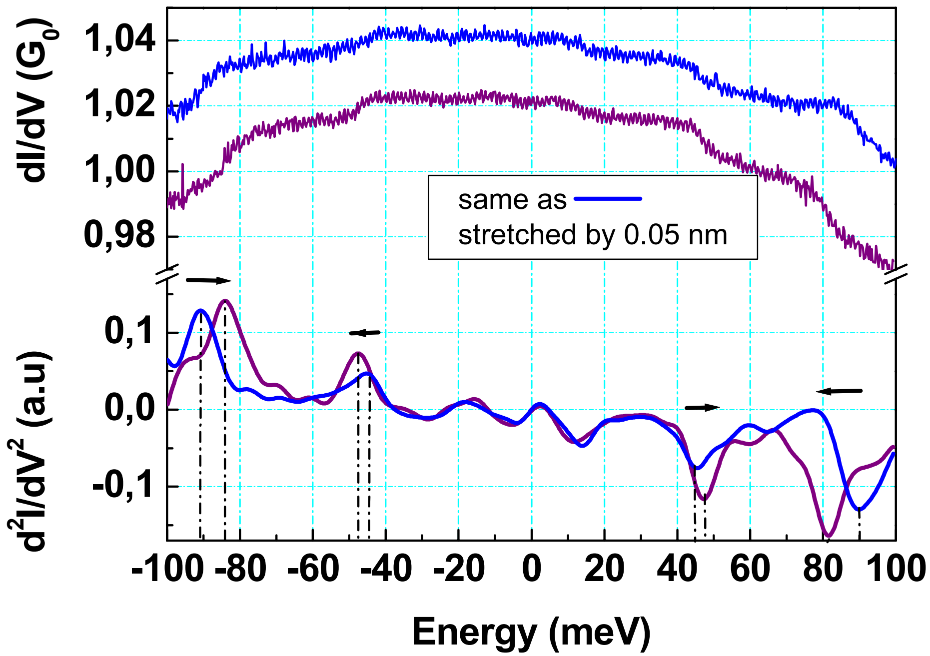

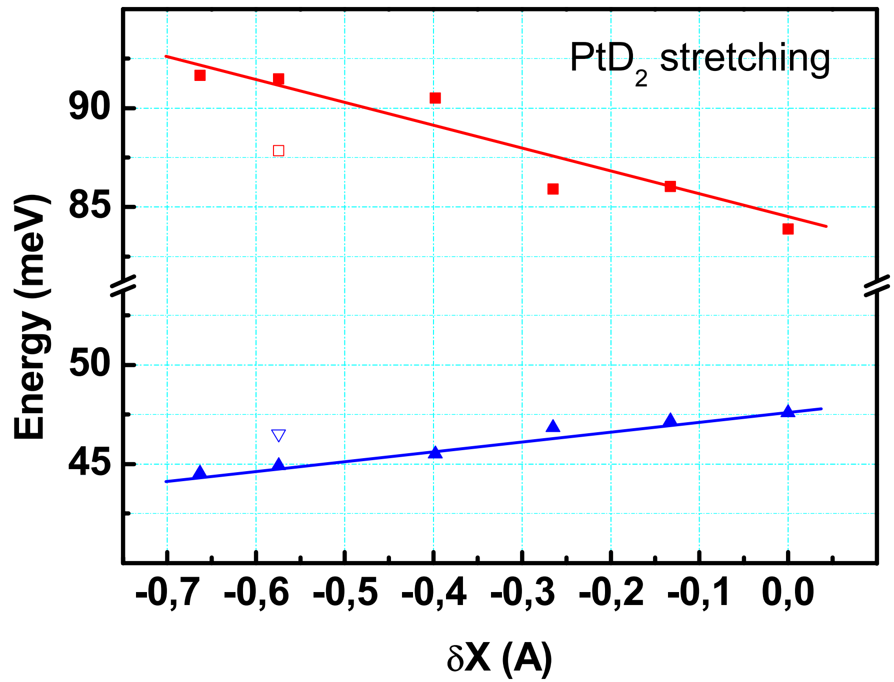

Casimir force: a force of nothing

$$\text{inside the cavity}: E=\sum_k \hbar\omega = \frac{\pi\hbar c}{L}\sum_{n=1}^{\infty} n$$

$$\text{outside the cavity}: E=\frac{\pi\hbar c}{L}\int_0^{\infty} n\,\mathrm{d}n$$

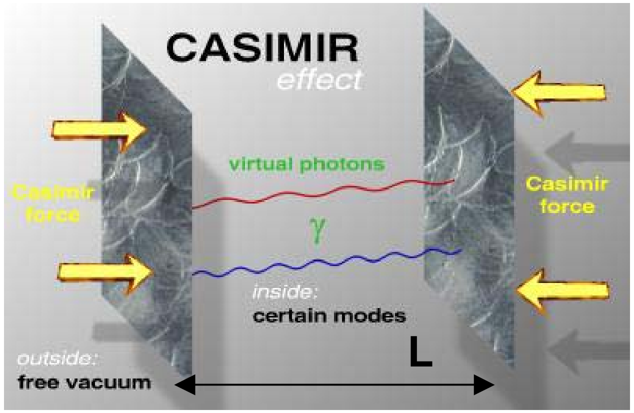

$$\Delta E=\frac{\pi\hbar c}{L}\left[\sum_{n=1}^{\infty} n-\int_0^{\infty} n\,\mathrm{d}n\right]$$

Euler - Maclauren :

$$\sum_{n=0}^{\infty} f(n)-\int_0^{\infty} f(n)\,\mathrm{d}n=\frac{1}{2}f(0)-\frac{1}{12}f'(0)+\frac{1}{720}f''(0)-\ldots\ldots$$

$$f(n) = n \Rightarrow f(0)=0, f'(0)=-\frac{1}{12},\ f''(0)=0$$

$$\Delta E=-\frac{\pi\hbar c}{12L} \Rightarrow \text{force} =\frac{\pi\hbar c}{12L^2}$$

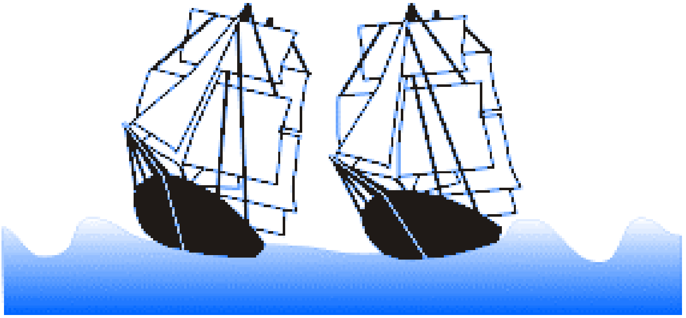

can be generalized to other geometries (3D, plate-sphere), temperature effects and non-ideal conductors

vacuum fluctuations: Casimir effect

In absence of electrostatic forces, attractive force between plate and sphere: $F \propto z^{-3}$

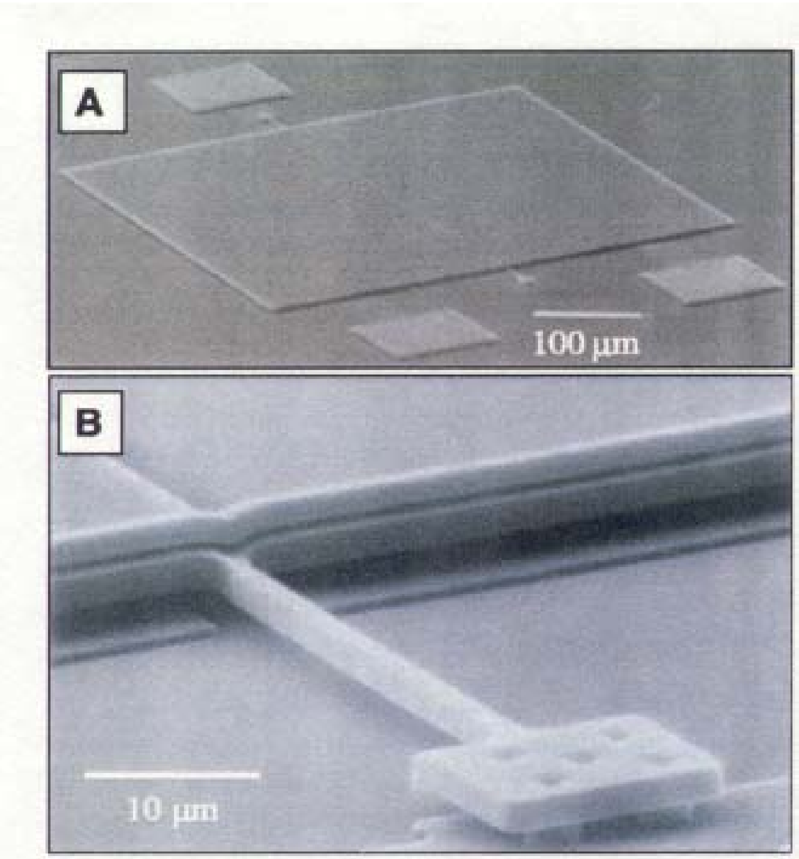

MEMS technology

(MicroElectroMechanical Systems)

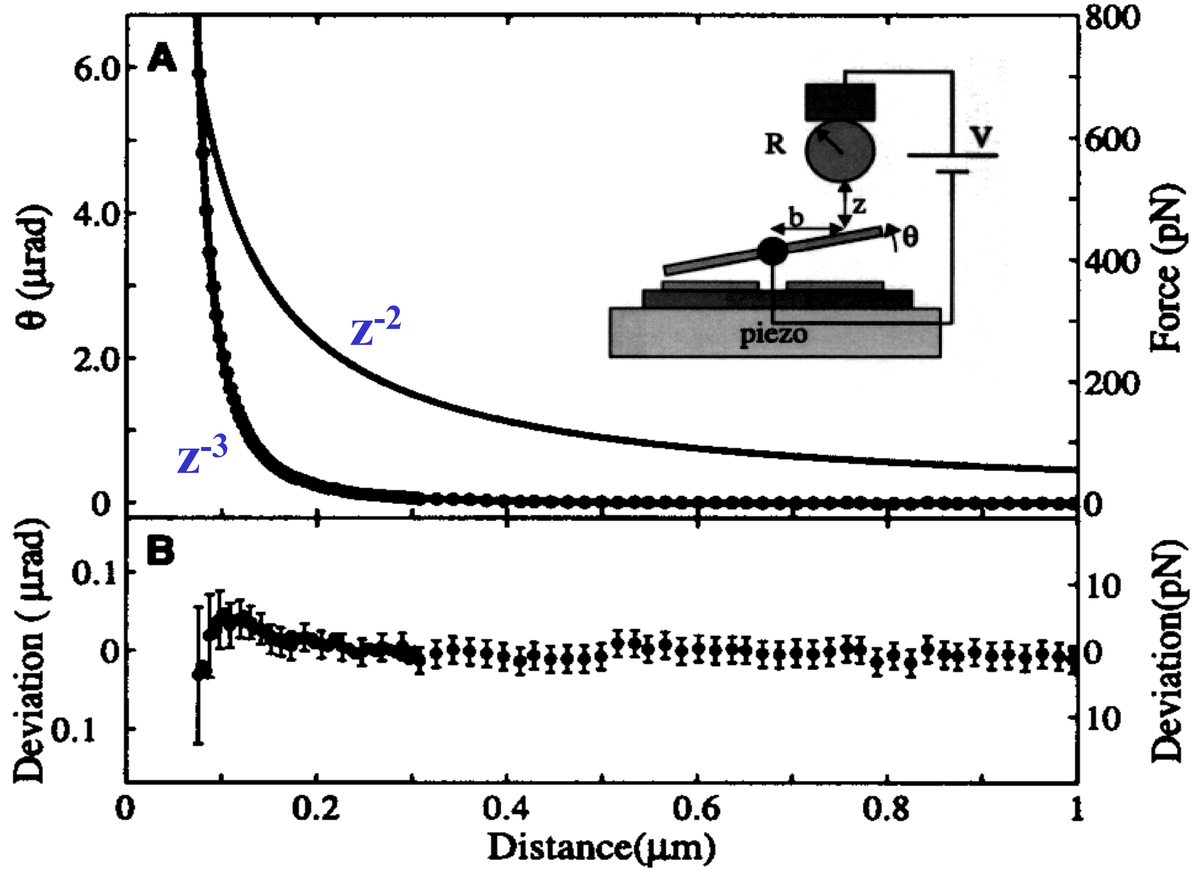

H.B. Chan et al., Science 291 (2001) 1941

mesoscopic phonons

Planck Distribution

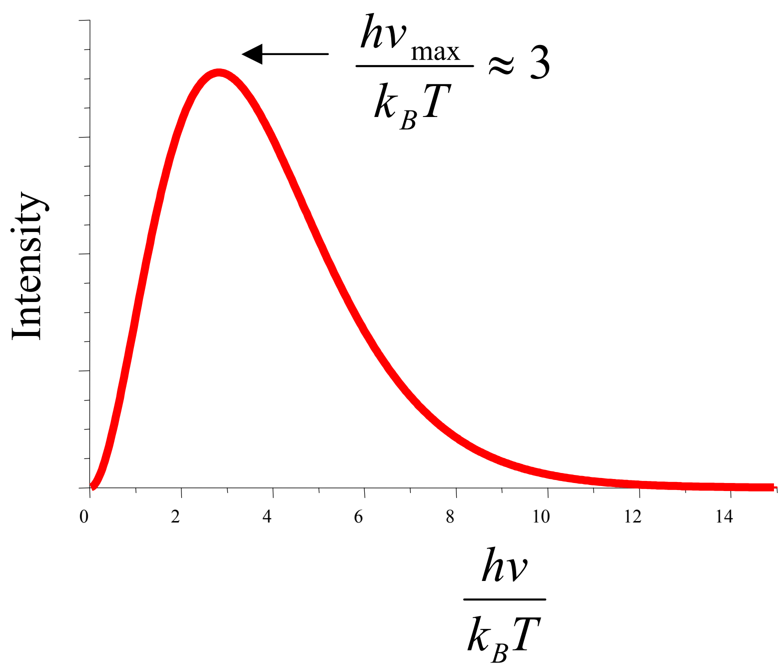

$$\lambda_{max} = \frac{c}{\nu_{max}} \approx \frac{hc}{3k_B T} = \frac{112nm}{T}$$

at 10K, $\boxed{\begin{aligned}\lambda_{max} &= 11nm \\ \nu_{max} &= 625GHz\end{aligned}}$

at 10 mK, $\boxed{\begin{aligned}\lambda_{max} &= 11\mu m \\ \nu_{max} &= 625MHz\end{aligned}}$

By nanofabrication techniques, we can enter domain where particle wavelength is comparable to channel dimensions.

Courtesy Keith Schwab

the thermal conductance "quantum"

derivation analogous to that of the electrical conductance quantum but look at the energy flux (instead of electron flux) and use Bose-Einstein statistics (consider two reservoirs with a T difference ΔT coupled by a 1D channel)

$$J = \hbar\omega\, n\, v$$

$$J = \int \frac{\mathrm{d}k}{2\pi} \hbar\omega(k)\,\eta(\omega)\,v(k) \qquad \eta(\omega) = \frac{1}{e^{\hbar\omega/k_B T} - 1}; \quad v(k) = \frac{\mathrm{d}\omega}{\mathrm{d}k}$$

$$J_{TOT} = \int_0^\infty \hbar\omega\left[\eta^+ - \eta^-\right]\mathrm{d}\omega \qquad \eta^+ - \eta^- = \tfrac{\partial\eta}{\partial T}\Delta T$$

$$G_{th} = \frac{J_{TOT}}{\Delta T} = \frac{\pi^2 k_B^2}{3h} T$$

the existence of a thermal conductance quantum also indicates that it is difficult to cool nano-objects to their ground state !!

Wiedemann-Franz law:
G_{th} = LGT, L= Lorentz constant
With $G_0 = e^2/h$ one finds $G_{th} = \pi^2 k_B^2 T/3h$

quantum phonon transport

$$g_0 = \pi^2 k_B^2\, T/3h$$

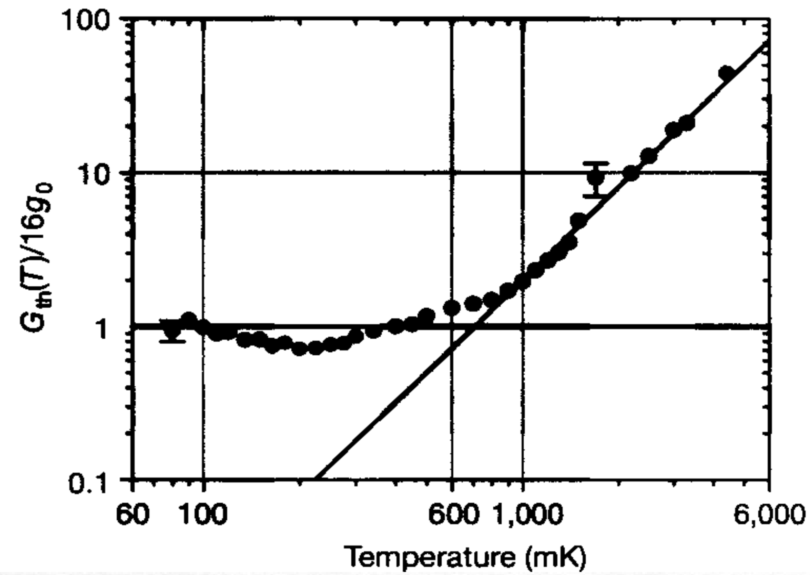

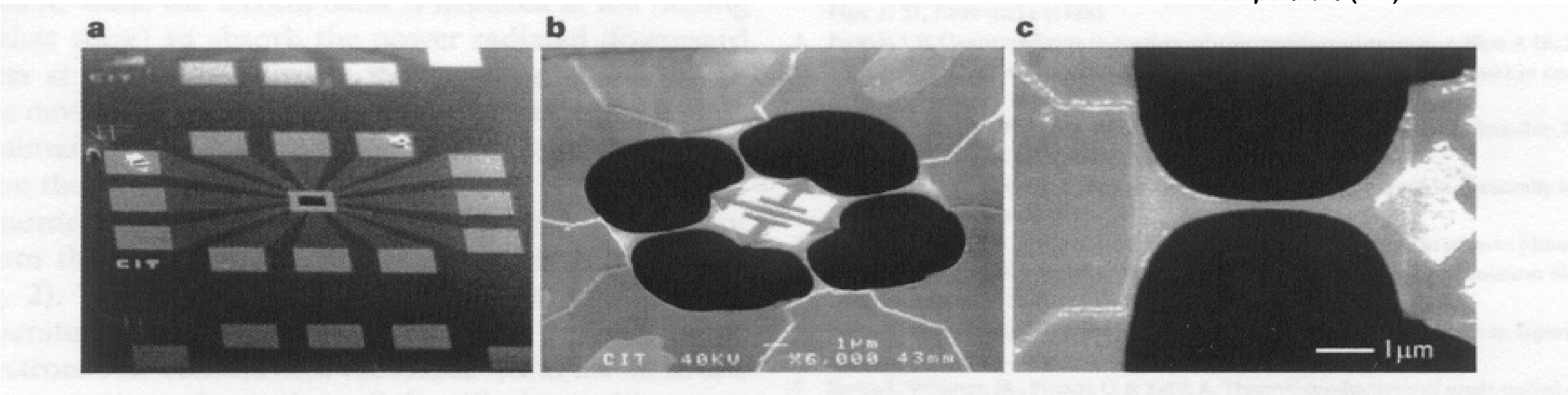

Schwab et al, Nature 404 (2000) 974

eigenfrequencies cantilevers and beams

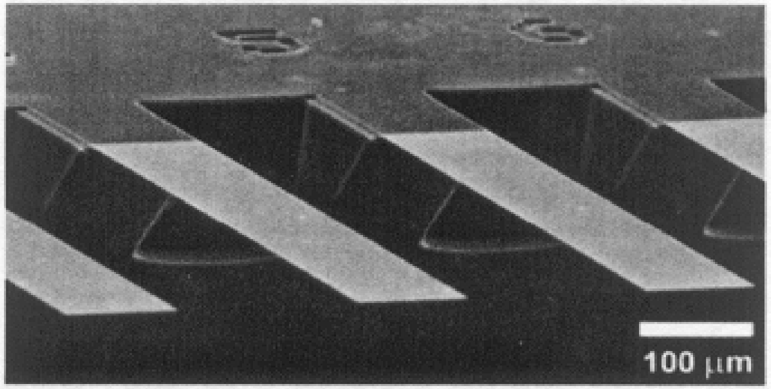

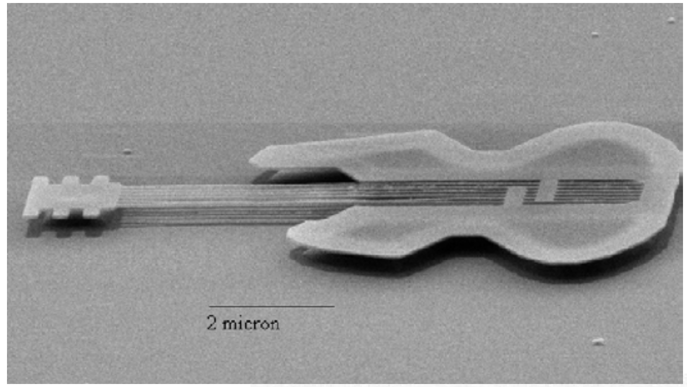

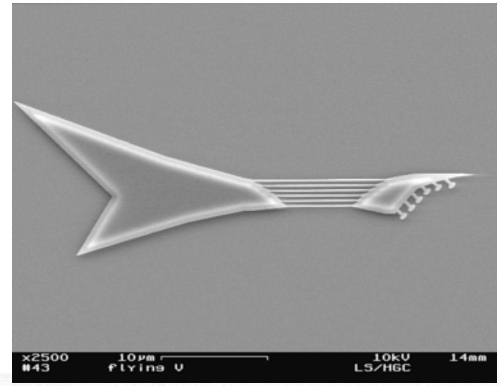

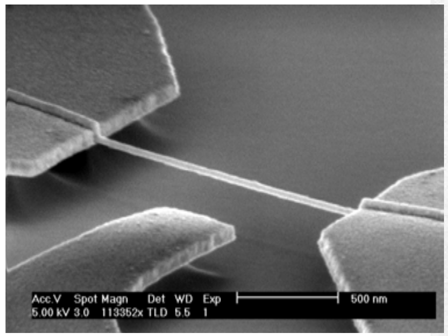

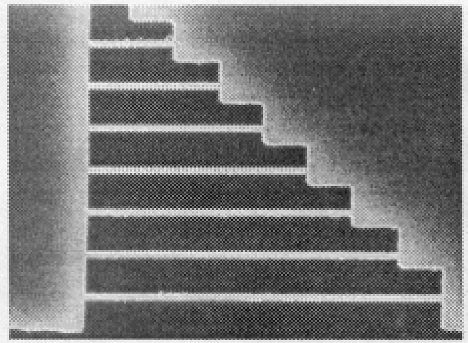

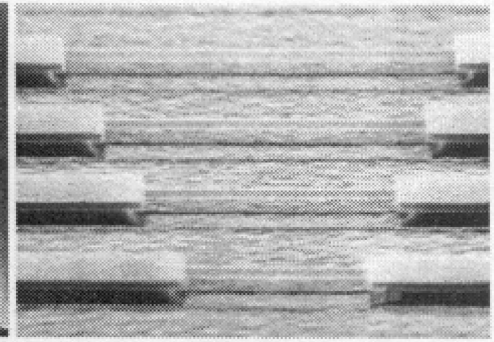

classical elasticity, Euler-Bernoulli theory:

$$\rho A \frac{\partial^2 u_y}{\partial t^2} + EI \frac{\partial^4 u_y}{\partial z^4} = 0, \qquad 0 < z < L$$

solve and use appropriate boundary conditions

top-down fabrication: surface nanomachining

1.
starting material: heterostructure with a single structural layer

2.
<u>mask definition</u>: by optical and e-beam lithography and thin film deposition

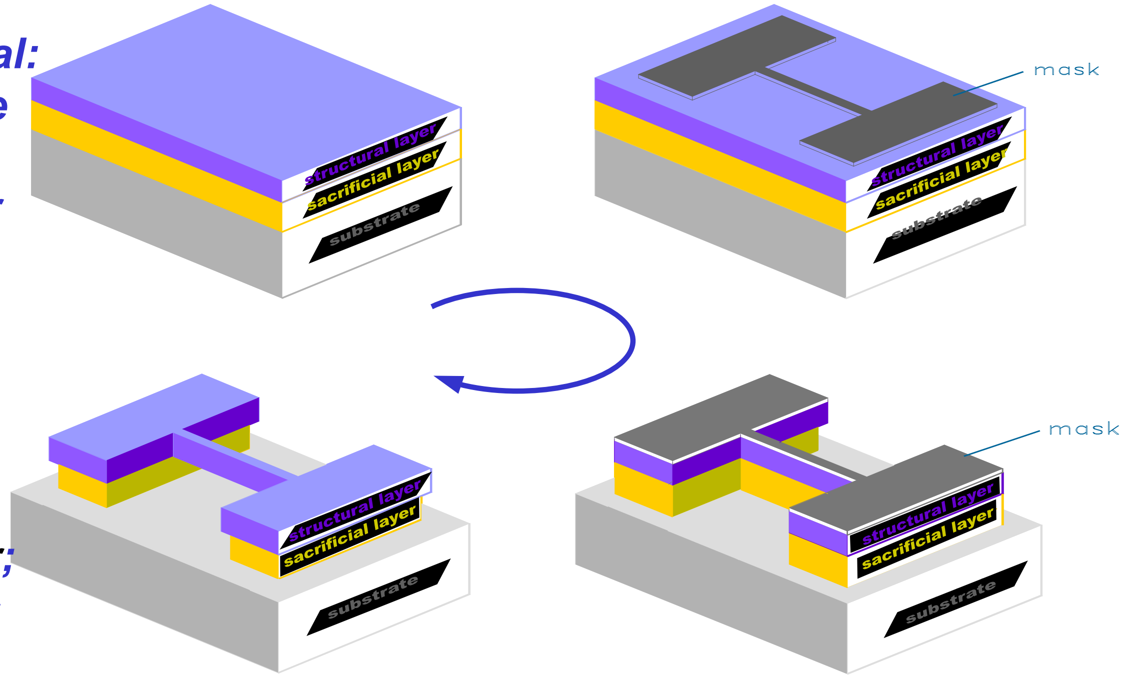

3.
<u>pattern transfer</u>: anisotropic etch defines structure vertically

4.
<u>selective etch</u>: removes the sacrificial layer; final structures are suspended

- *high resolution e-beam lithography (x,y)*
- *mono-crystalline epitaxial layers (z)*
- *GaAs-based systems*
- *Si-based systems (SOI)*
- *Silicon Carbide*

eigenfrequencies cantilever

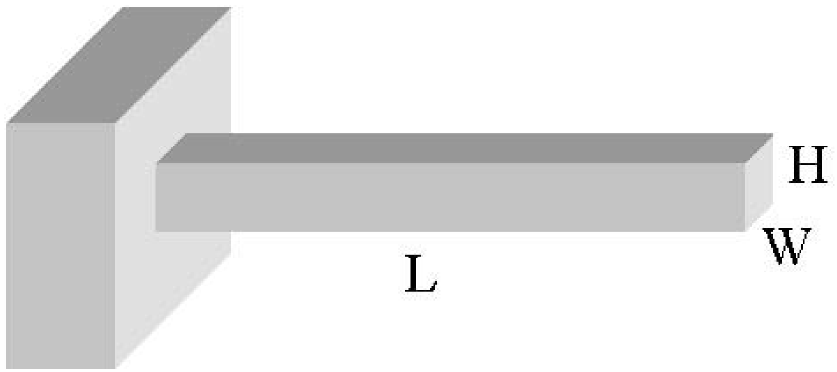

$$\xi(0) = \xi'(0) = 0$$
$$\xi''(L) = \xi'''(L) = 0$$

$$I = \frac{WH^3}{12} \Rightarrow f_n = \frac{\alpha_n^2 H}{2\pi L^2}\sqrt{\frac{E}{12\rho}}$$

boundary conditions:

$$1 + \cosh(kL)\cos(kL) = 0$$

$$\alpha_n = k_n L;\ \alpha_1 = 1.8751,\ \alpha_2 = 4.6941,\ \ldots\ldots,\ \ \alpha_n = \frac{\pi}{2}(2n-1)$$

for the first modes: not harmonic

sound velocity: $v = (E/\rho)^{1/2}$

eigenmodes of cantilever nanotube

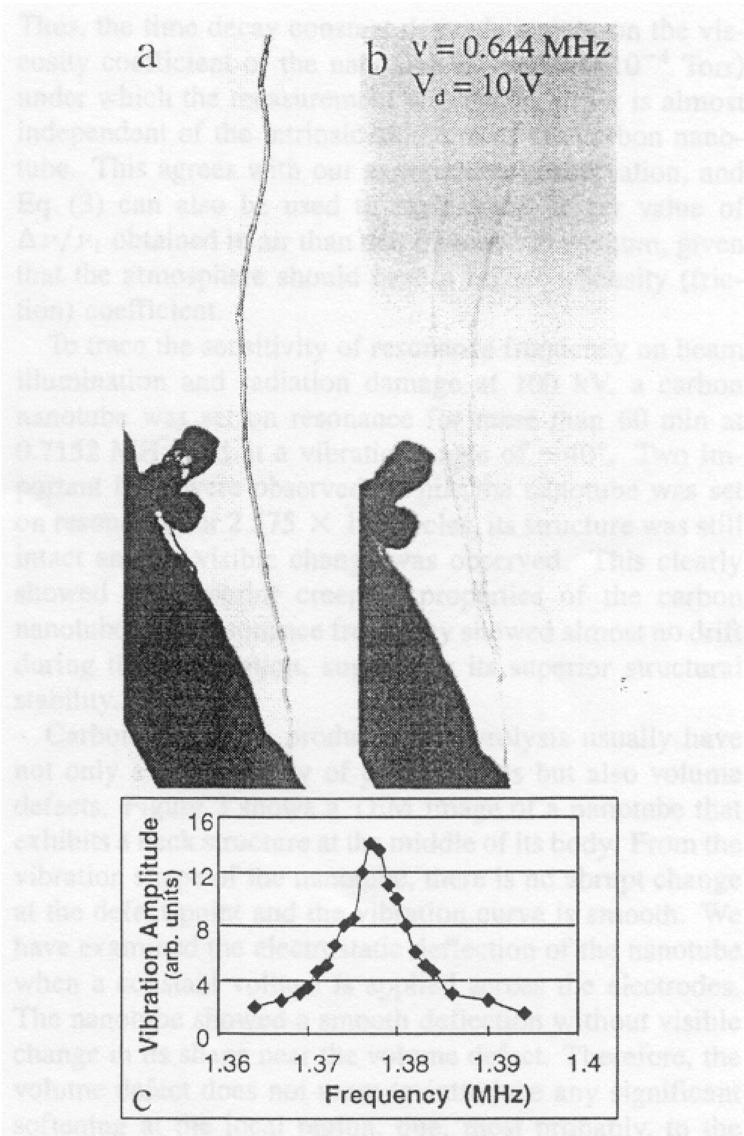

TEM work: Gao et al, PRL 85 (2000) 622

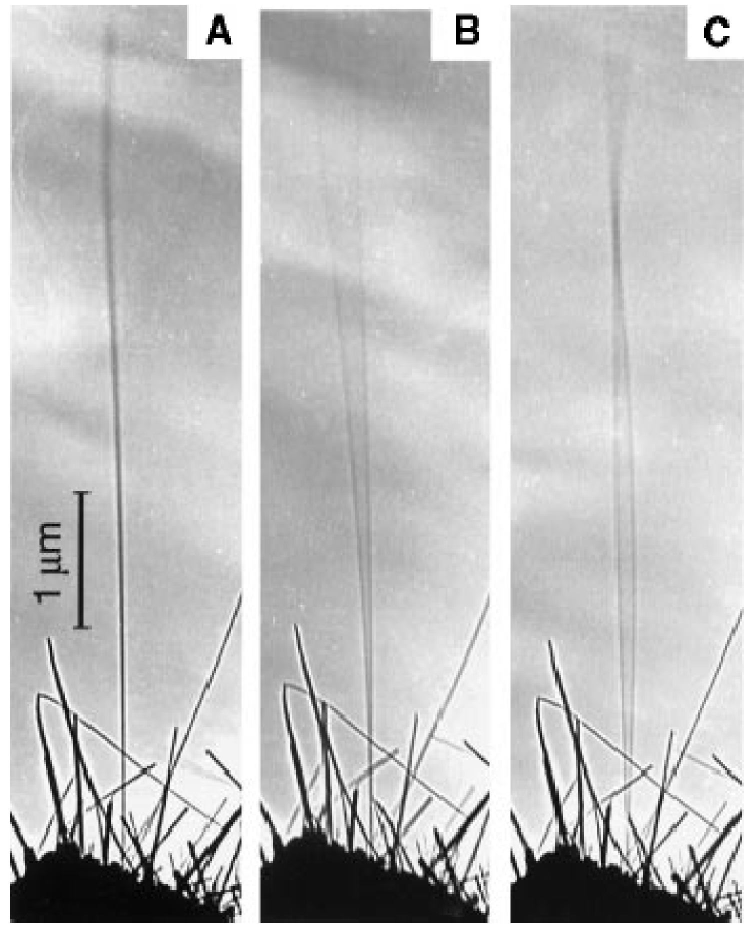

P. Poncheral et al., Science 283 (1999) 1513

eigenfrequencies double clamped beams

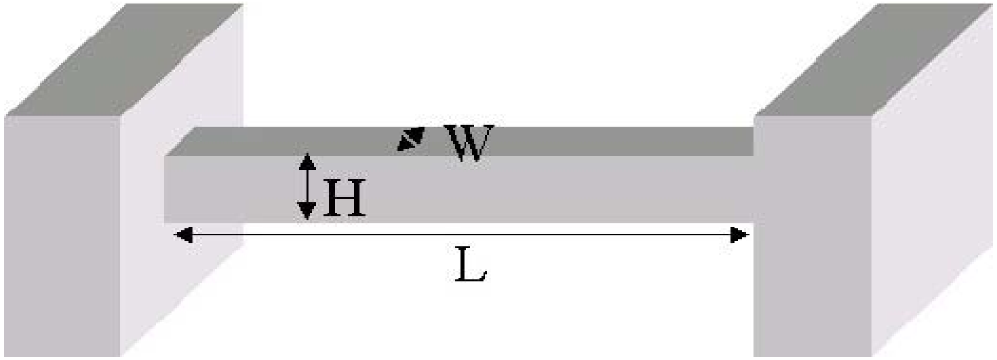

$$\xi(0) = \xi'(0) = 0$$
$$\xi(L) = \xi'(L) = 0$$

$$I = \frac{WH^3}{12} \Rightarrow f_n = \frac{\beta_n^2 H}{2\pi L^2}\sqrt{\frac{E}{12\rho}}$$

boundary conditions:

$$1 - \cosh(k_n L)\cos(k_n L) = 0$$

$$\beta_n = k_n L;\ \ \beta_1 = 4.7300,\ \beta_2 = 7.8532,\ \ldots\ldots,\ \ \beta_n = \frac{\pi}{2}(2n+1)$$

silicon:
L=1 μm, H=W=0.1 μm, f_0= 1GHz

nanotube:
L= 100 nm, d = 1.4 nm, f_0= 5 GHz

double clamped strings/beams

$$EI\frac{\partial^4 u}{\partial z^4} - T\frac{\partial^2 u}{\partial z^2} - K = 0$$

APL 78 (2001) 162

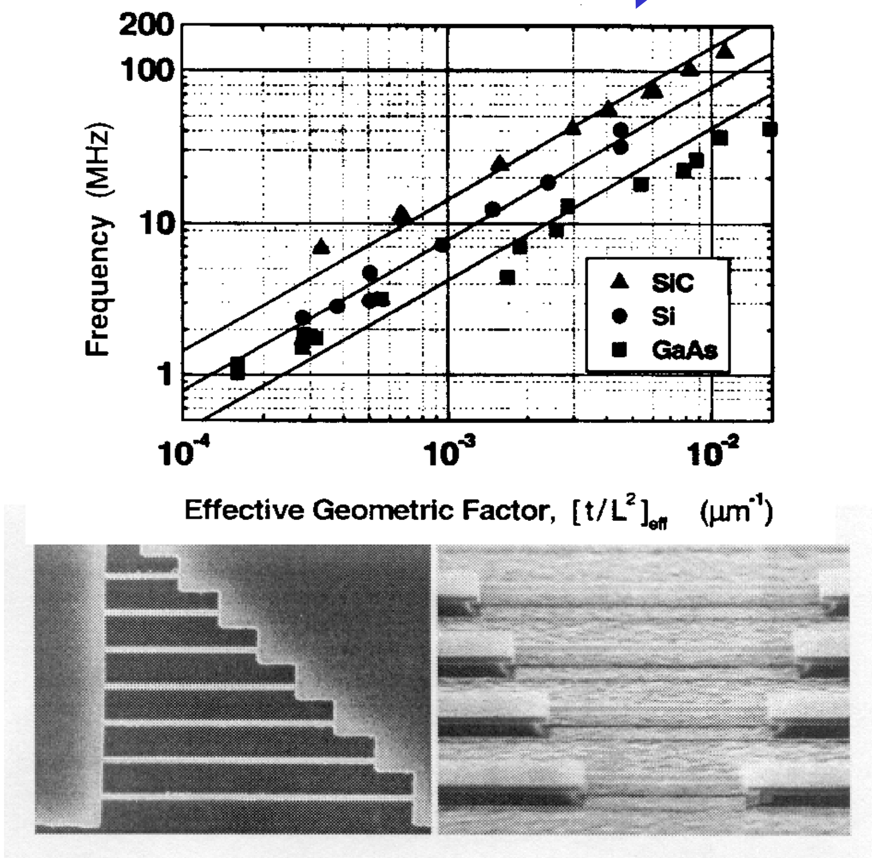

frequency $\propto$ L^{-2}

frequency $\propto$ L^{-1}

magnetomotive method: conducting beam (50 Ω)

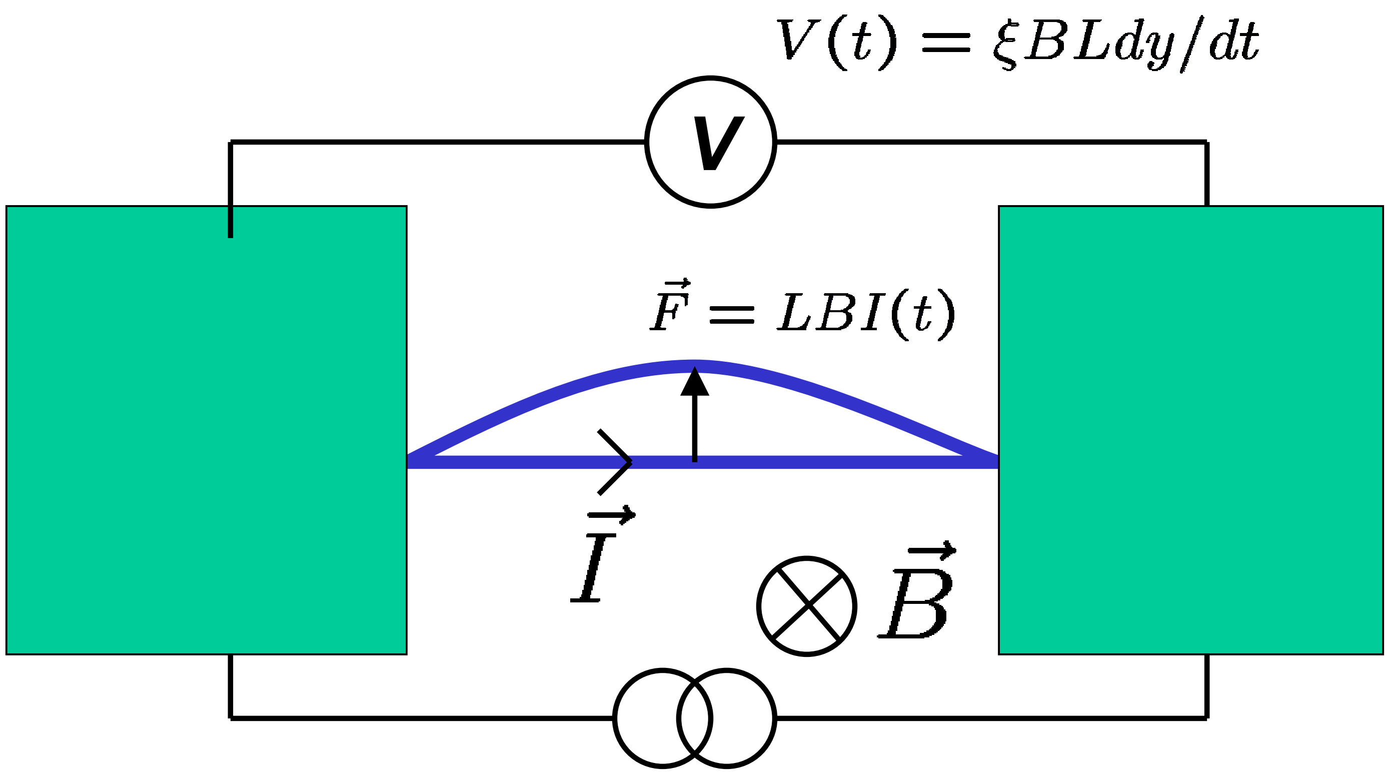

$F(t) = m\ddot{y} + \alpha\dot{y} + ky = BLI(t)$ assume $\alpha^2 \ll mk$

amplitude at resonance $y_0 = QBLI_0/k$

$$V_0 = \xi BL y_0 \omega_0 = \xi Q B^2 L^2 I_0 \omega_0 / k = \frac{\xi Q B^2 L^2}{m\omega_0} I_0 \equiv R_m I_0$$

$\xi = 0.83$, depends on bending profile

Cleland and Roukes, Sensors and Actuators 72, 256 (1999)

example of a measurement

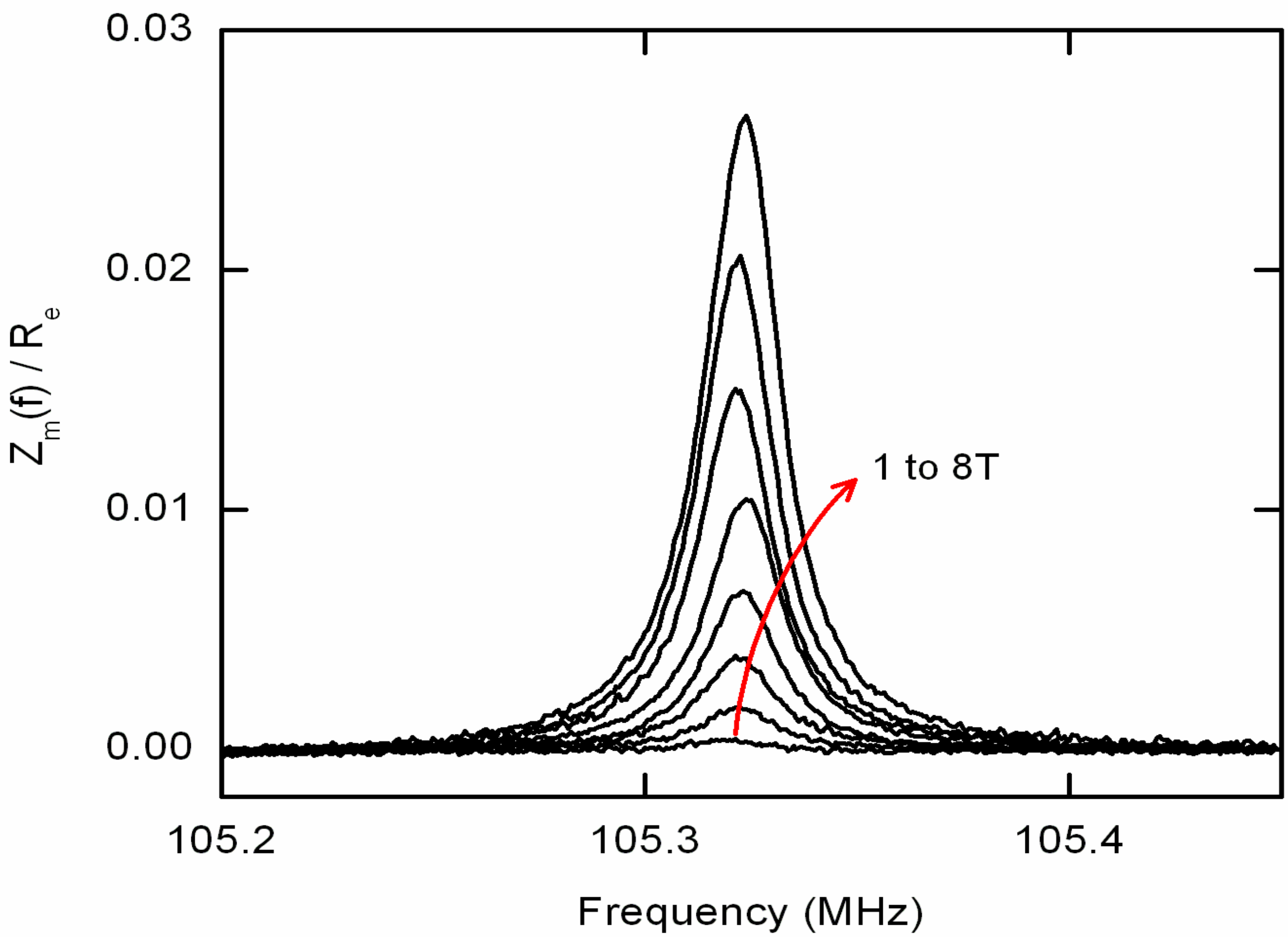

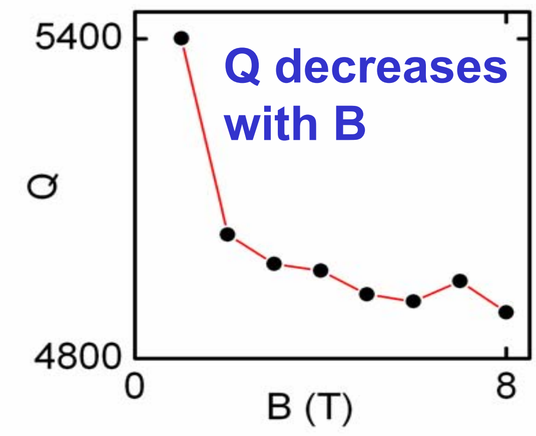

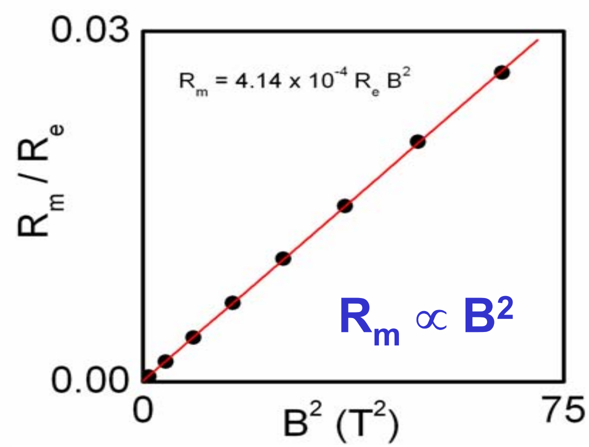

For Q > 10: response of the damped, driven the same as that of a harmonic oscillator. Lorentzian peak shape; the width defines the Q-factor.

increasing drive: nonlinear response (Duffing oscillator)

"Jimmy Hendrix regime"

$$F_{eff} = kx + k'x^3$$

$$x_c = \frac{2d}{\sqrt{Q/2(1-\nu^2)}}$$

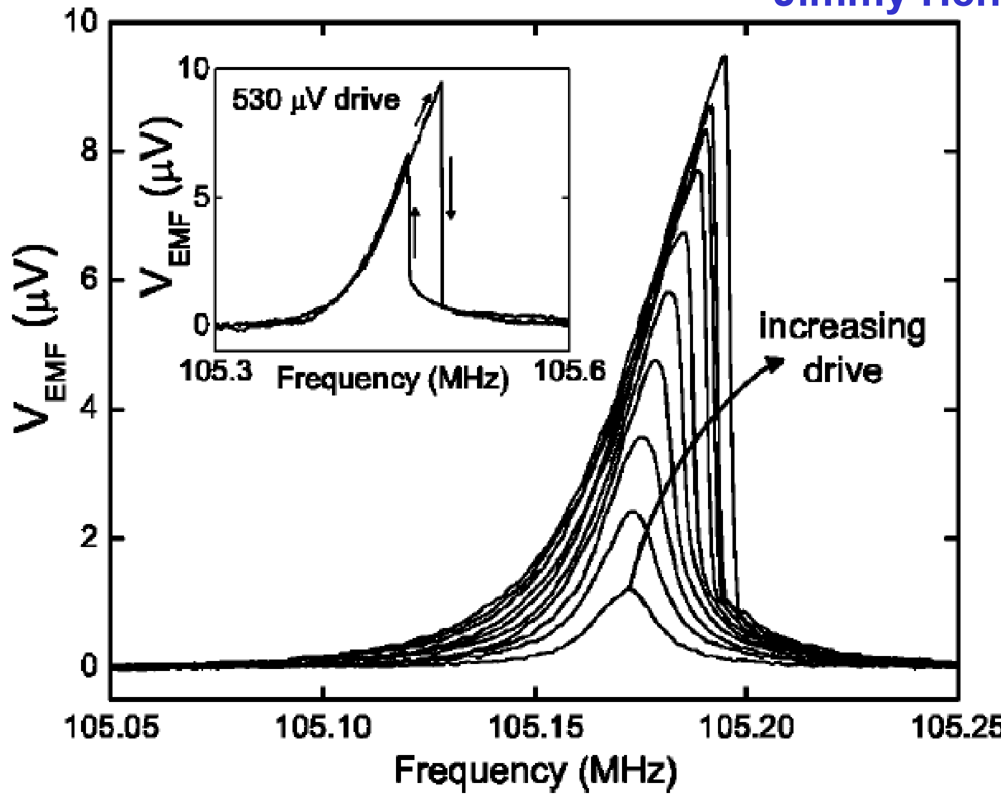

Husain et al, APL 83 (2003) 1240

interesting for applications (parametric amplification) and for new quantum effects (Thorwart et al. (2005))

quantum-limited detection of motion

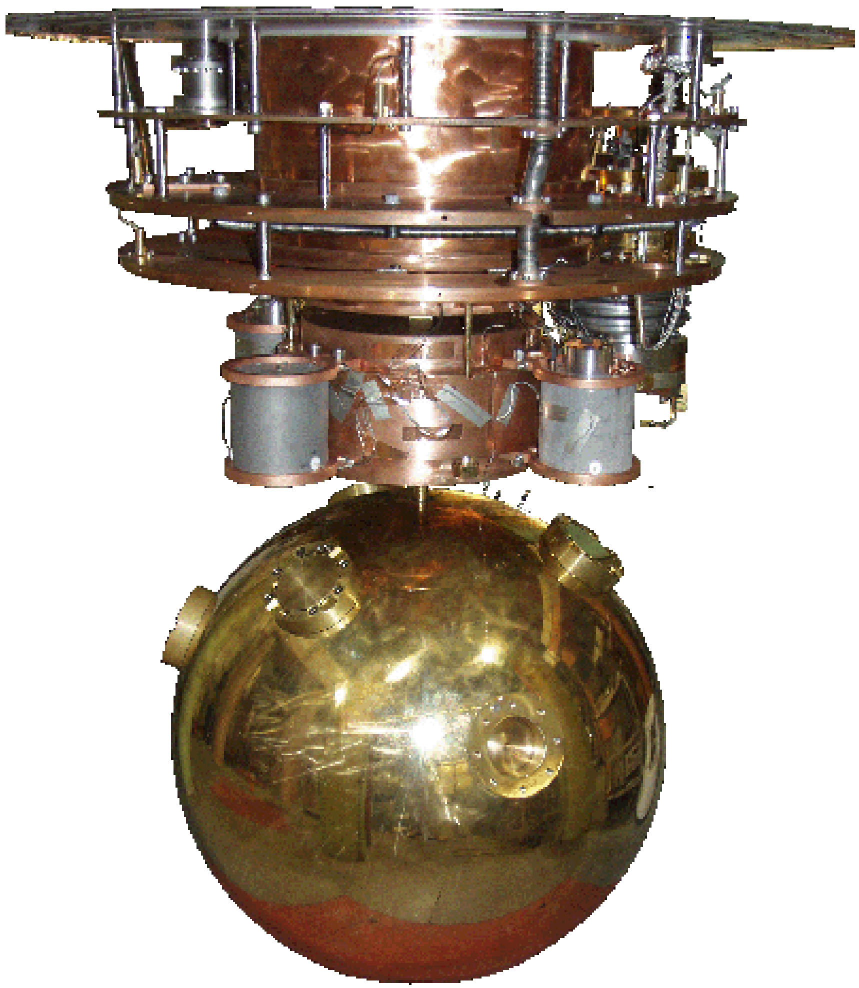

detection of gravitational waves

The MiniGRAIL detector is a cryogenic 68 cm diameter spherical gravitational wave antenna made of CuAl(6%) alloy with a mass of 1400 Kg, a resonance frequency of 2.9 kHz and a bandwidth around 230 Hz, possibly higher. The quantum-limited strain sensitivity dL/L would be ~4×10^{-21}. The antenna will operate at a temperature of 20 mK. An other similar detector is being built in São Paulo, which will strongly increase the chances of detection by looking at coincidences. The sources we are aiming at are for instance, non-axisymmetric instabilities in rotating single and binary neutron stars, small black-hole or neutron-star mergers etc.

MiniGRAIL: Frossati (Leiden University)

quantum effects in a harmonic oscillator

$$H = \frac{1}{2}kx^2 + \frac{1}{2}\frac{p^2}{m}$$

$$\Rightarrow E_n = \hbar\omega\left(n + \frac{1}{2}\right)$$

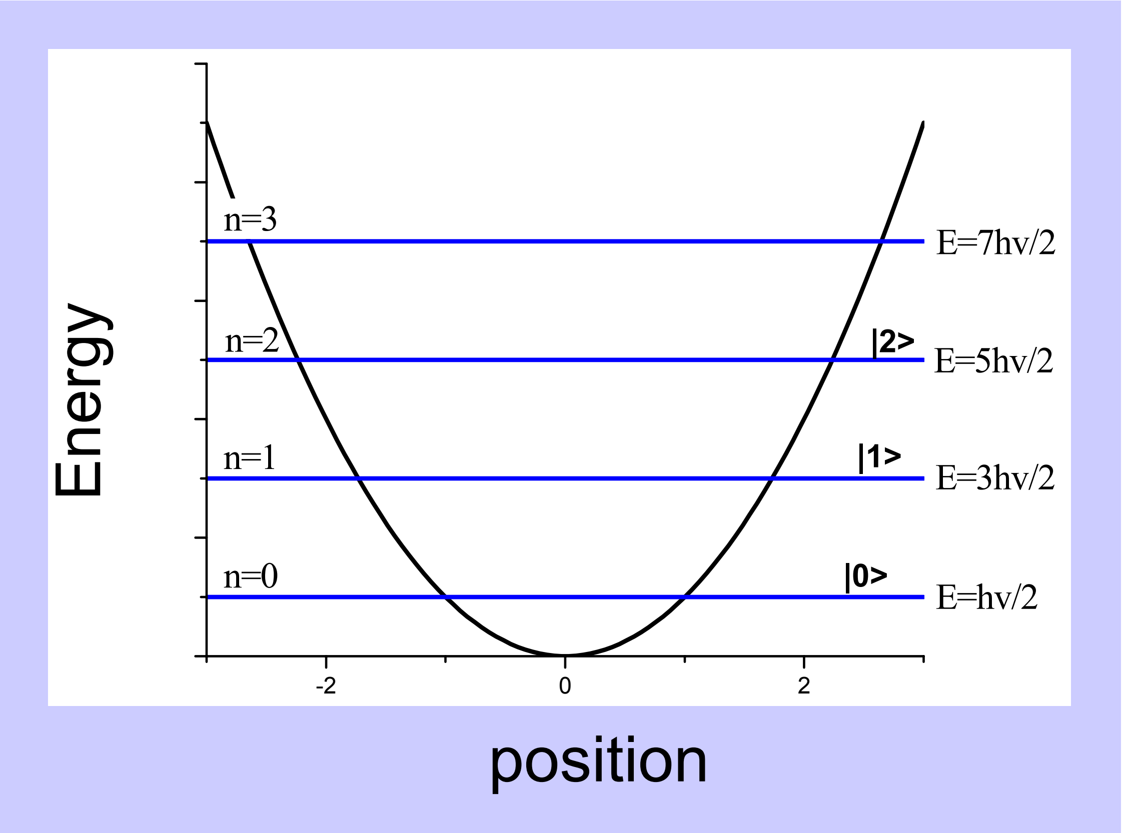

zero-point motion:

$$x_0 = \sqrt{\frac{\hbar}{m\omega_0}}$$

energy stored in the oscillator: $\langle E \rangle = \frac{\hbar\omega}{2} + \frac{\hbar\omega}{e^{\hbar\omega/k_B T} - 1}$

quantum regime if occupation number (N_{th}) is of order one: 1 GHz $\Rightarrow$ T_{sample} < 50 mK

zero point motion

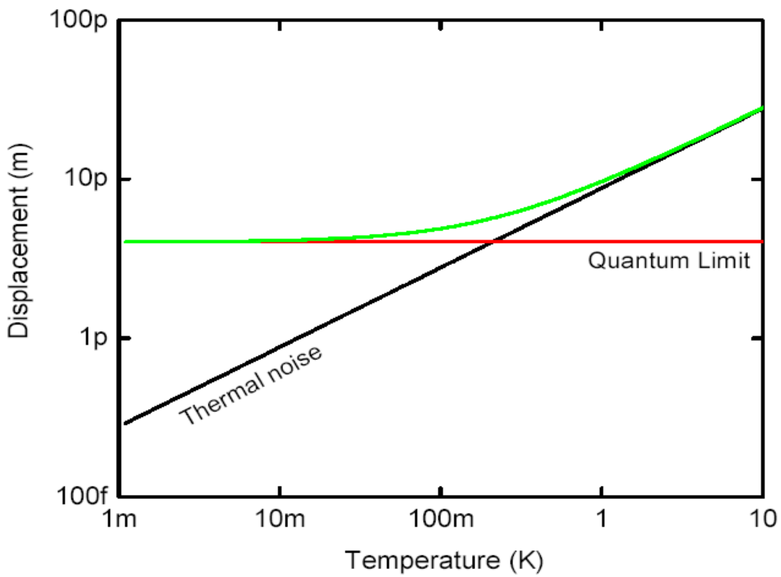

expected rms displacement noise of a 4.4 GHz nanotube resonator as a function of temperature

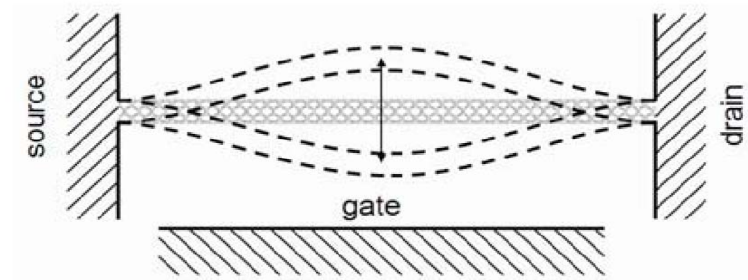

needed: high Q; high frequency, low mass

MEMS devices as electrometers

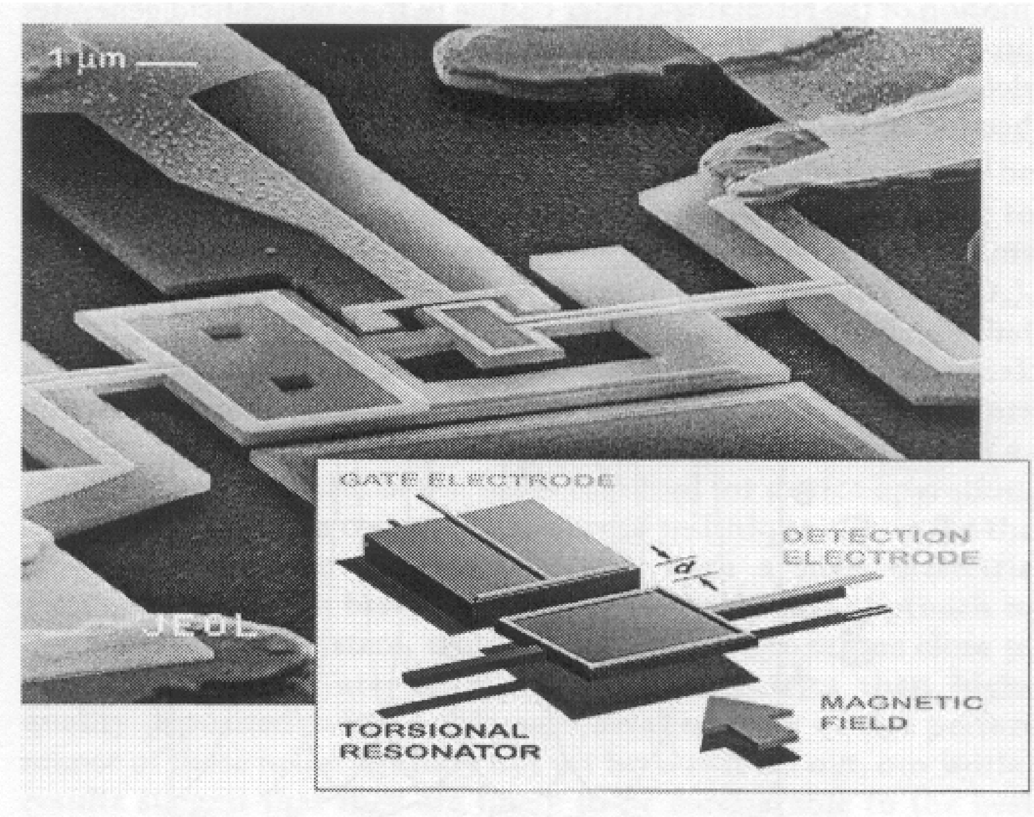

•measured sensitivity (300 K): 0.1 eHz$^{-1/2}$

•ultimate sens. (300 K): 2 x 10 $^{-5}$ eHz$^{-1/2}$

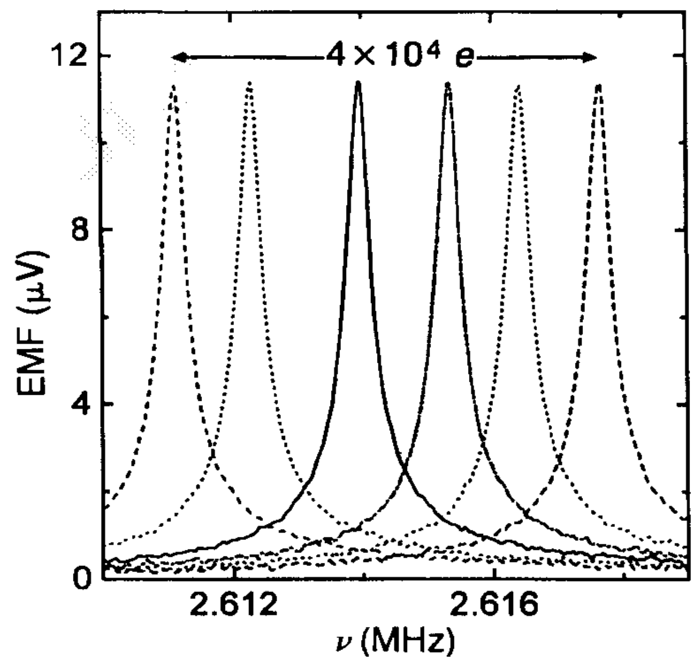

Cleland and Roukes, Nature ***392*** *(1998) 160*

<u>towards</u> zero-point motion detection using a SET and a mixing technique

$$x_0 = \sqrt{\frac{\hbar}{m\omega_0}}$$

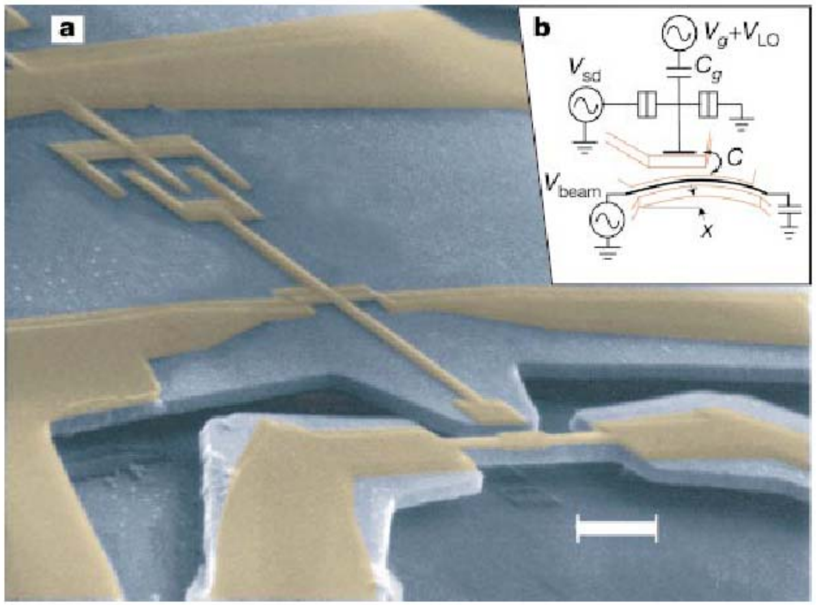

Figure 1 The device used in the experiment. **a**, Scanning electron micrograph of the device, showing the doubly clamped GaAs beam, and the aluminum electrodes (coloured) forming the single electron transistor and beam electrode. Scale bar, 1 μm. The $Al/AlO_x/Al$ tunnel junctions have approximately $50 \times 50\ nm^2$ overlap. **b**, A schematic of the mechanical and electrical operation of the device.

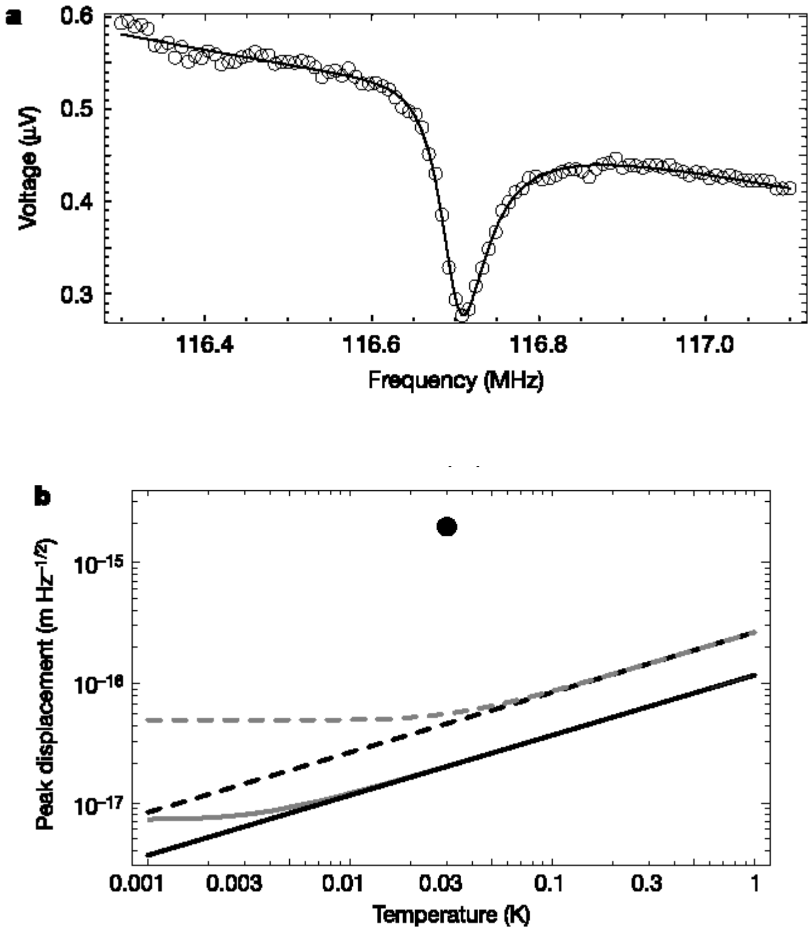

x_0 a factor 100 above the quantum limit; N_{th} = 10

Knobel and Cleland, Nature 424 (2003) 291

almost quantum detection limit with RF-SET

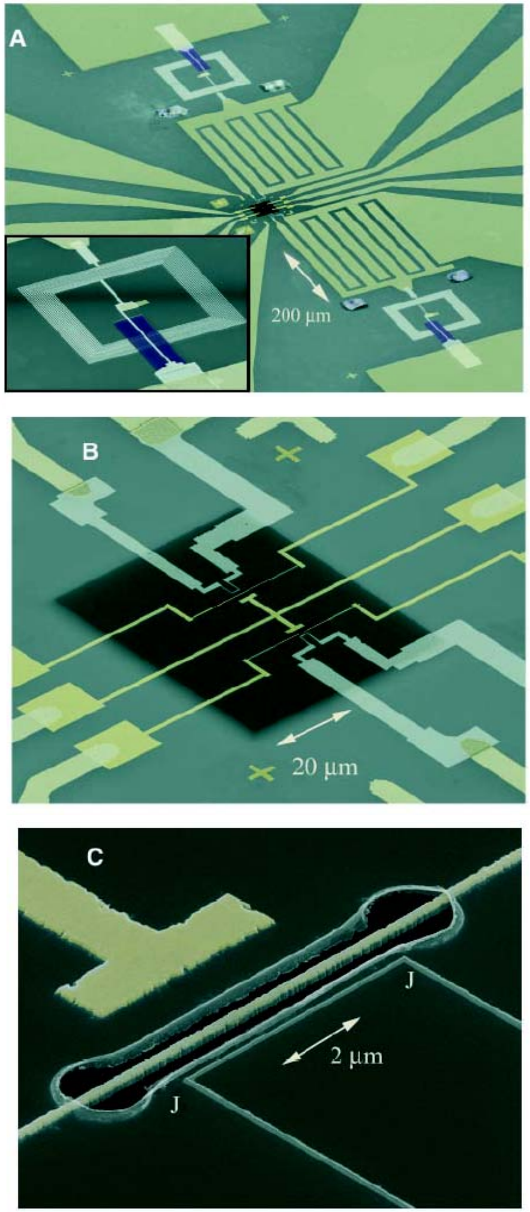

x_0 a factor 4.3 above the quantum limit; N_{th} = 58

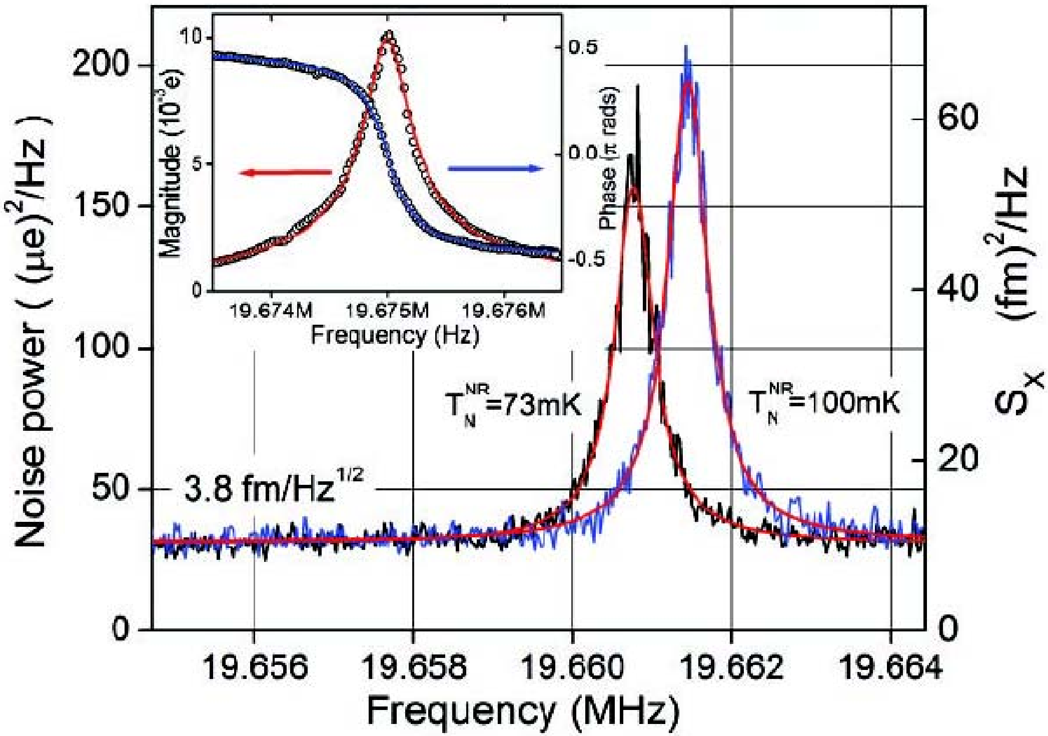

Fig. 3. Charge noise power around the mechanical resonance with V_{NR} = 15 V. Right peak is taken at 100 mK and is fit with a Lorentzian, shown as a red line. This noise power is used to scale the left peak taken with the refrigerator at 35 mK and corresponds to a resonator noise temperature of T_N^{NR} = 73 mK. This then scales the white-noise floor, which corresponds to a system-noise temperature of T_N^{SSET} = 16 mK = 18 T_{QL}. Using the equipartition relation, the displacement resolution is 3.8 fm/$\sqrt{\text{Hz}}$. The inset shows the driven response, approximately 800 pm on resonance, with the data as circles and a Lorentzian fit as the solid lines. All SSET measurements are taken with the SSET biased near the double Josephson quasiparticle resonance peak.

$$\frac{1}{2}k_B T = \frac{1}{2}m\omega^2 x_{RMS}^2$$

LaHaye et al., Science 304 (2004) 74

Coulomb blockade in SET that can move

• usual CB theory does not apply since the gate capacitance is distance dependent

• mechanical degrees of freedom via classical theory of elasticity

• nanotube modeled as an elastic rod

• applicable to other suspended structures

• nanotube: hope for high Q-factors (smooth on a nanometer level)

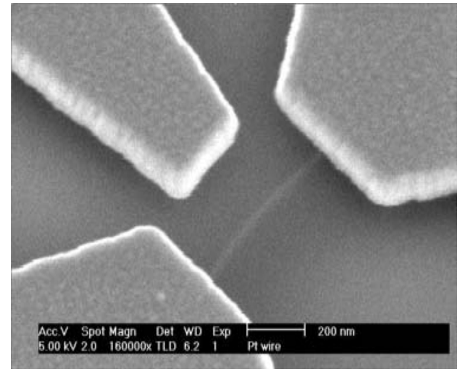

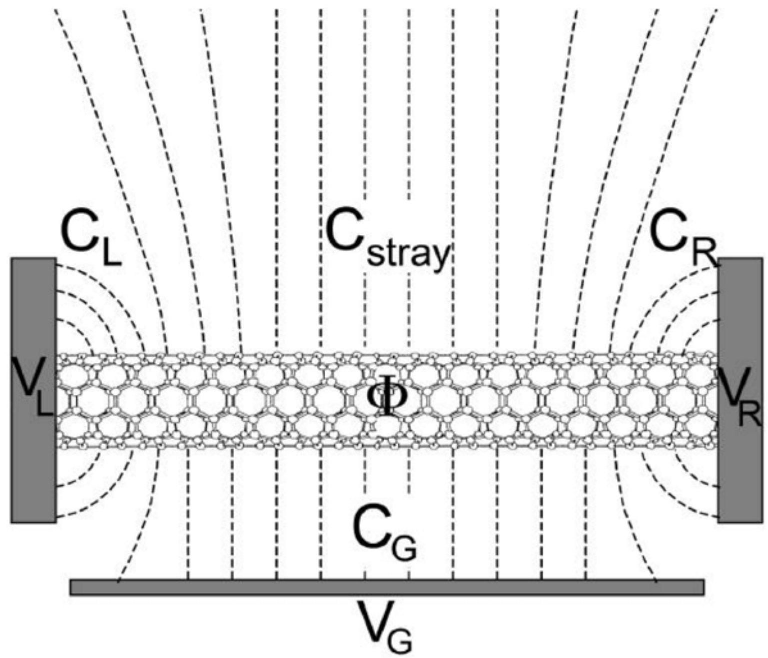

S. Sapmaz et al., PRB ***67*** *(2003) 235414*

bottom-up fabrication: suspended nanotubes

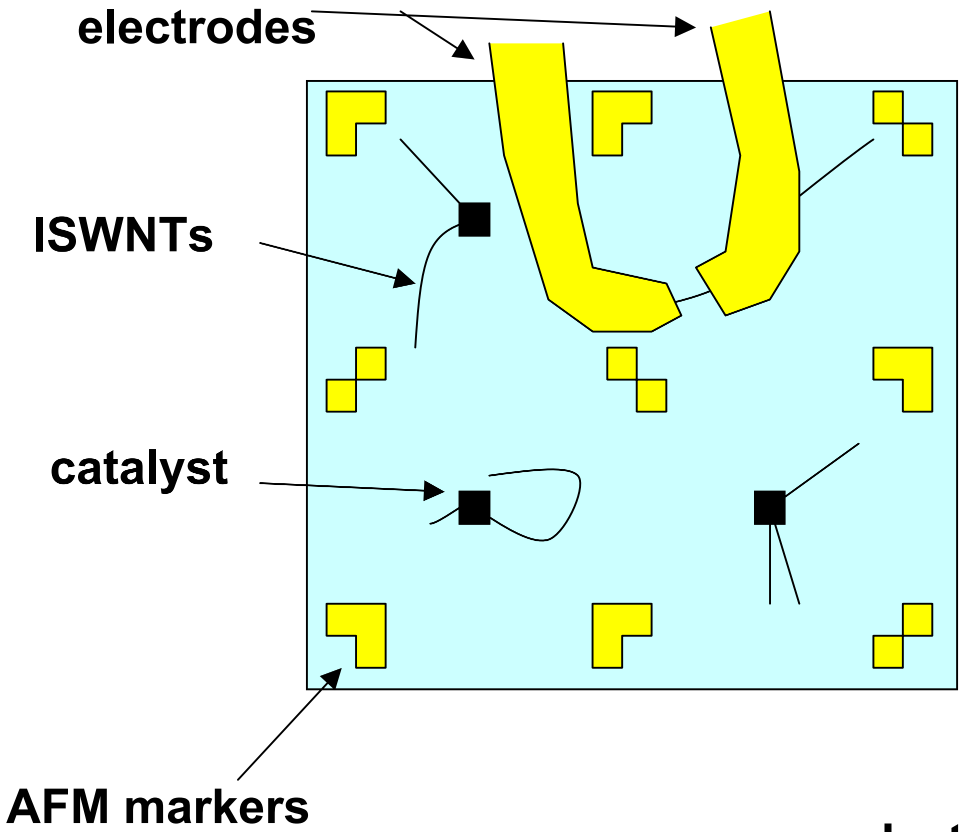

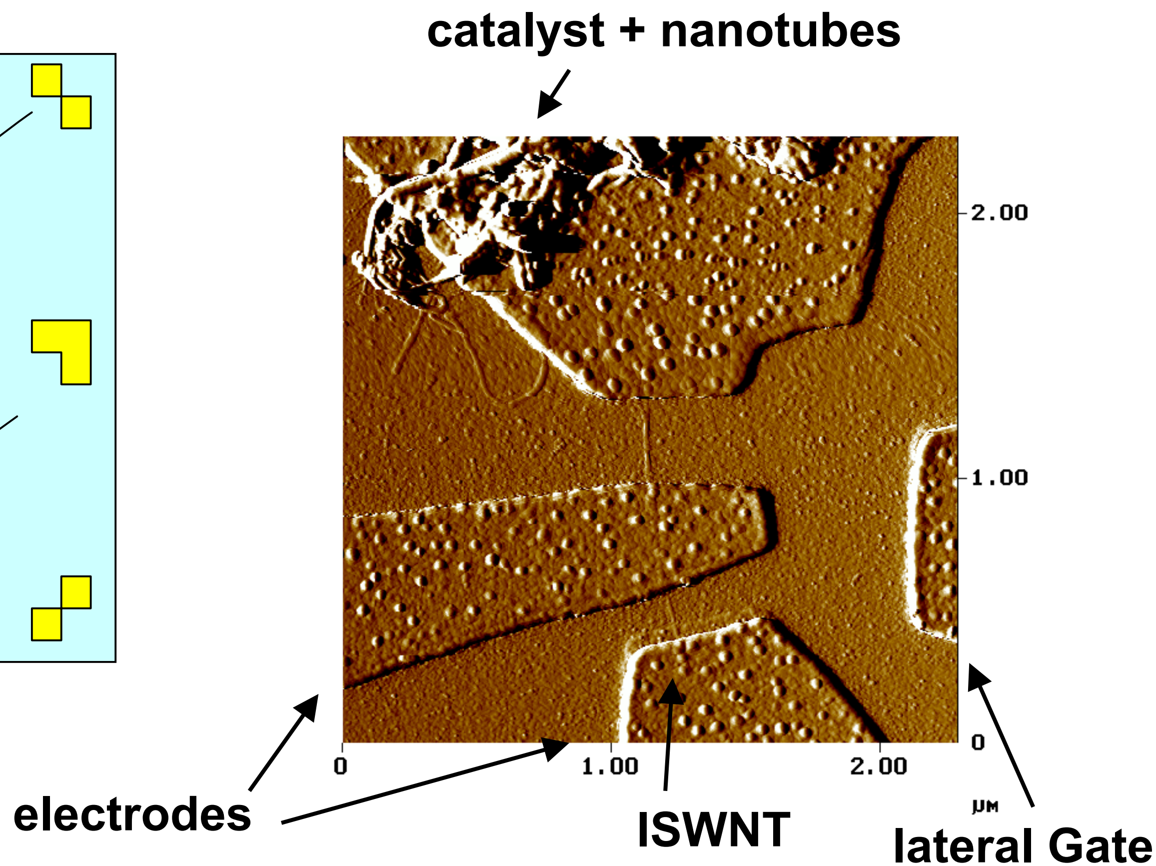

bottom-up fabrication: suspended nanotubes

before etching

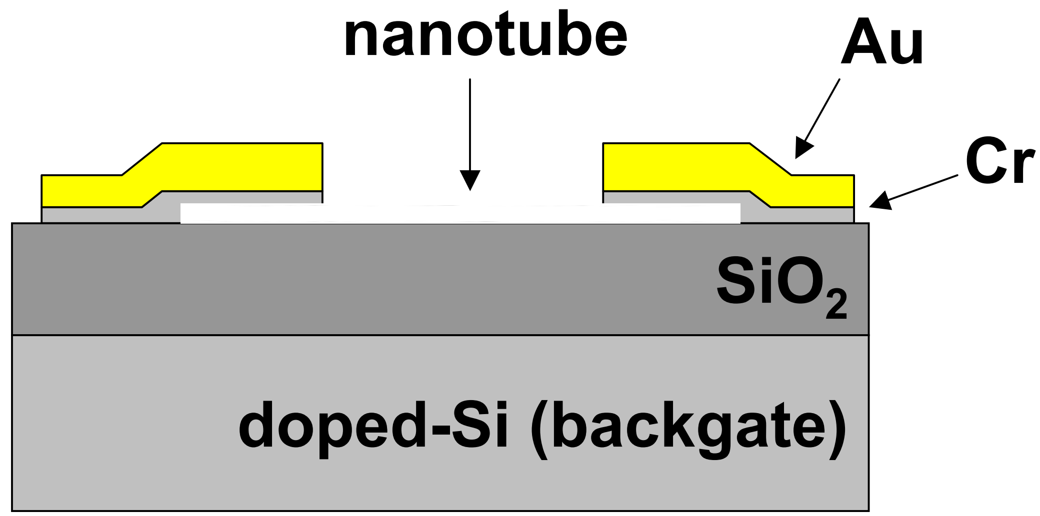

after etching
in acid (BHF)

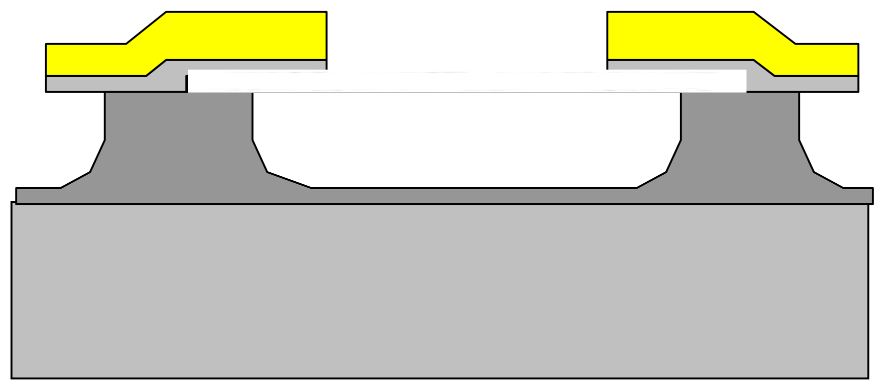

Nygård and Cobden, APL 79 (2001) 4216

electrostatic term in Coulomb Blockade is displacement dependent

$$W_{\text{el-st}}(z[x]) = \frac{(ne)^2}{2C_\Sigma} - neV_G$$

analytical case : $C_{\text{L}} = C_{\text{R}} = 0$

$$C_G(z[x]) = \int \frac{dx}{2\ln\left[\frac{2(R-z)}{r}\right]}$$

$$W_{\text{el-st}}(z[x]) = \frac{(ne)^2}{2C_0} - neV_G - \frac{(ne)^2}{L^2 R}\int z[x]\,dx$$

Electrostatic force (z<<R) : mechanical correction proportional to $(ne)^2$

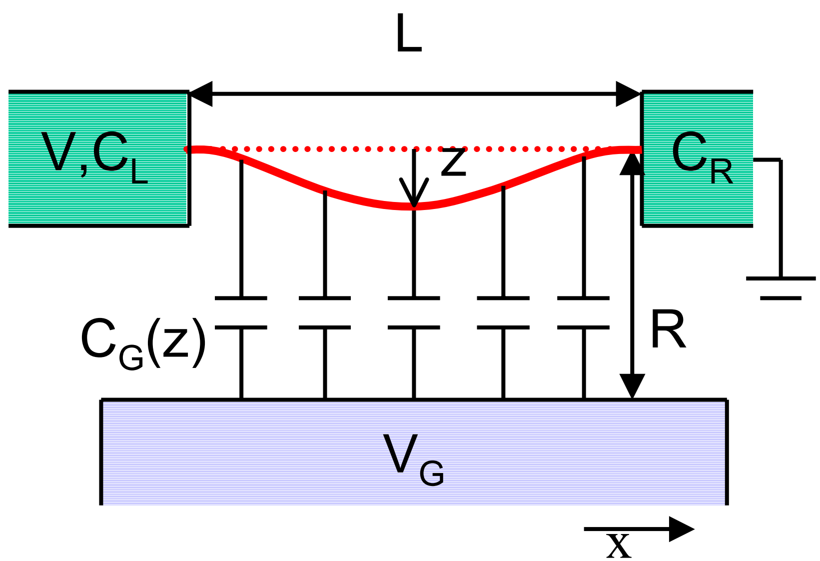

$$W \neq \frac{(ne+Q)^2}{2C_\Sigma}$$

the nanotube moves in discrete steps every time an additional electron tunnels onto it

weak bending:
$z_{max} < r$, $z_{max} \propto V_G^2$

strong bending:
$z_{max} > r$, $z_{max} \propto V_G^{2/3}$

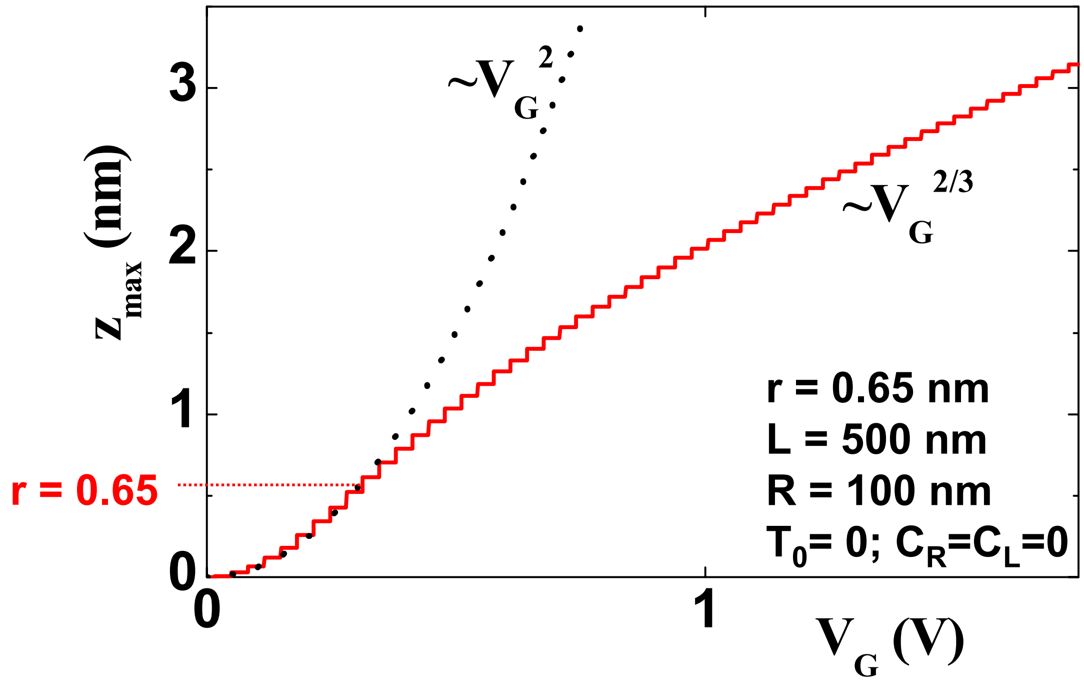

*S. Sapmaz et al., PRB **67** (2003) 235414*

As soon as z_{max}>d, the strain due to deformation has to be taken into account

electron-vibron coupling in a movable dot

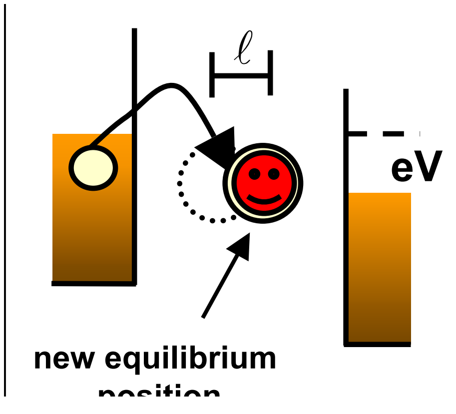

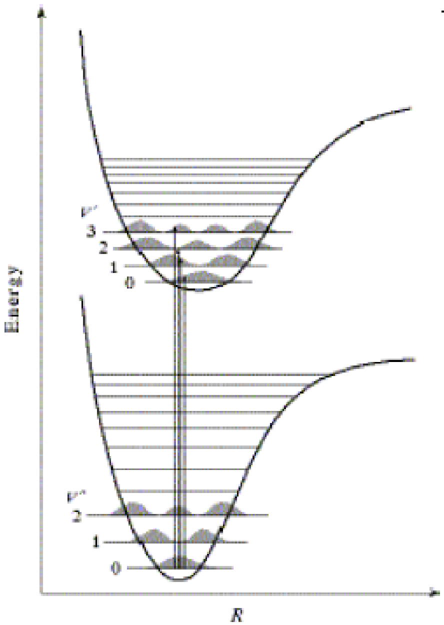

Frank-Condon factors: overlap between the harmonic oscillator wave functions in the initial ground state and the displaced final electronic state

$$\hat{H} = \frac{p^2}{2m} + \frac{1}{2} m \omega_0^2 x^2 + \lambda x$$

λ: e-ph coupling

$$g = \tfrac{1}{2}\lambda^2 = \tfrac{1}{2}\left(\frac{\ell}{\ell_0}\right)^2 \qquad \ell_0 = \sqrt{\frac{\hbar}{m\omega}}$$

$$\Gamma_{L,R} \Rightarrow \Gamma_{L,R} \left|\langle \Psi_{\text{after}} | \Psi_{\text{before}} \rangle\right|^2 = \Gamma_{L,R} P_{nm}$$

Frank - Condon factors determine step heights in IV

$$P_{n0} = \left|\langle \Psi(x-\ell) \,|\, \Psi(x) \rangle\right|^2 = \frac{e^{-g} g^n}{n!}$$

in practice: steps visible if g > 0.1

Braig and Flensberg, PRB 68 (2003) 205323

Frank-Condon factors reproduce step heights in the experiment reasonably well

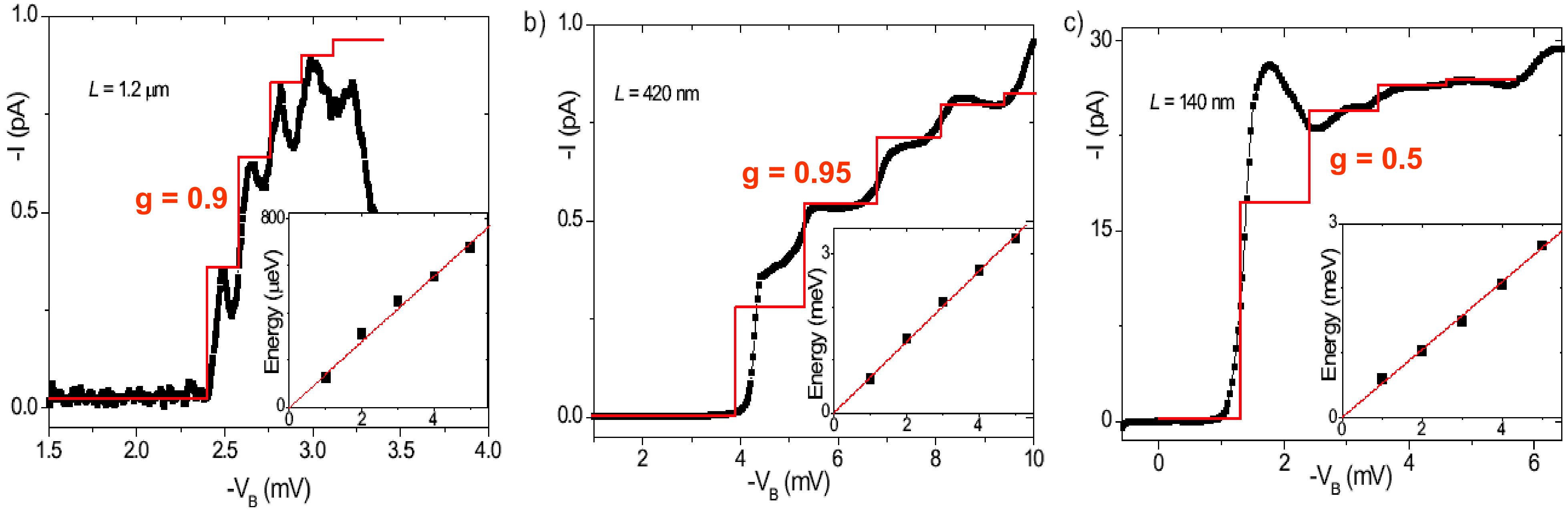

e-ph coupling constant is about 1 and approximately length and gate independent: displacement ~1 pm !

a nanotube of 1 micron length acts as a single quantum harmonic oscillator ($\hbar\omega >> k_B T$) !!!

A better fit may be obtained if the influence of a gate voltage and asymmetric coupling is considered (Braig and Flensberg, 2003) or if non-equilibrium phonons are present (Mitra, Aleiner and Milles, 2004); Negative Differential Resistance not understood

some vibrational modes nanotubes

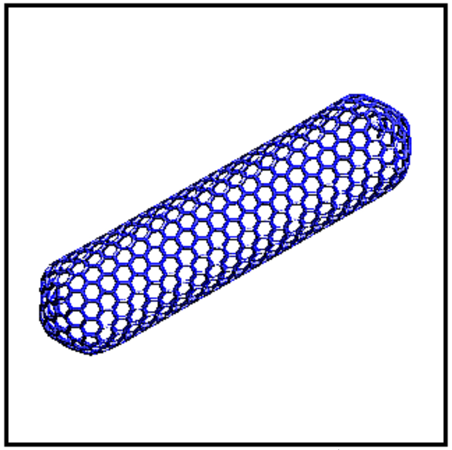

bending mode

f~2.5 GHz-25 MHz (100 nm-1 μm)
E~10-0.1 μeV

Length dep.

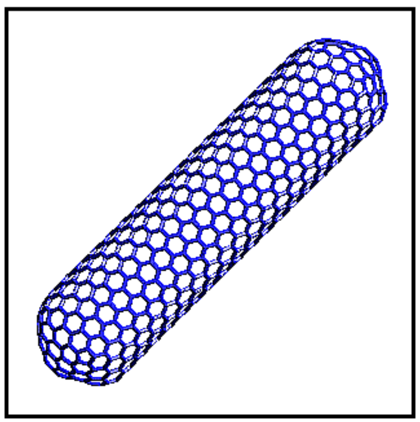

stretching (longitudinal) mode

f~1.3-0.13 THz (100 nm-1 μm)
E~600-60 μeV

squashing mode

f~0.54-1.0 THz,
E~2.2-4.2 meV

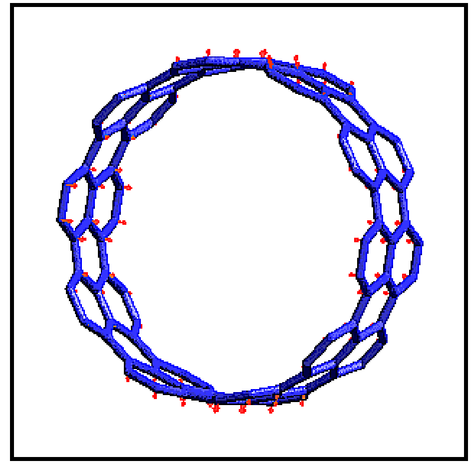

Length indep.

radial breathing mode

f~4.5-6.2 THz
E~18-25 meV

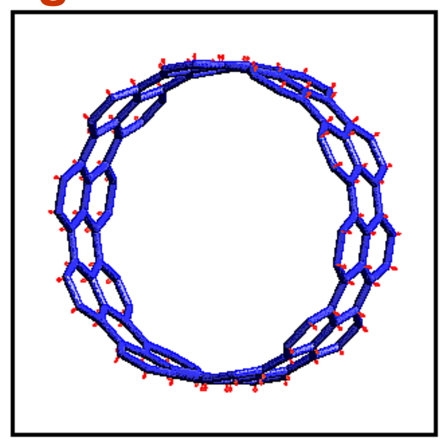

data fit longitudinal (stretching) modes the best

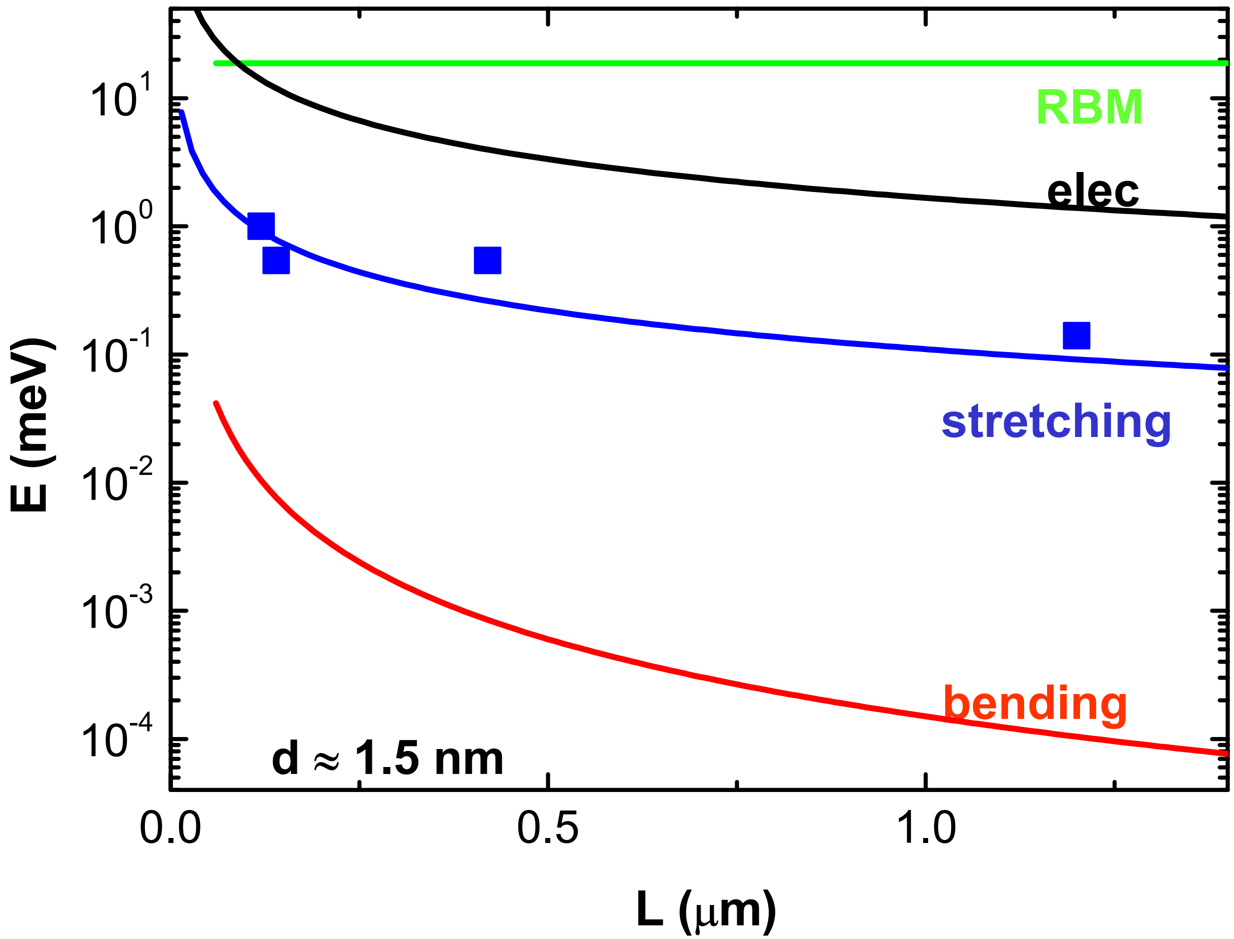

E = 18.7 meV

E = 1.67 meV L[μm]$^{-1}$

E = 110 μV L[μm]$^{-1}$

E = 0.1 μV L[μm]$^{-2}$

Sapmaz et al. PRL 96 (2006) 26801